Desalination and Water Treatment
www.deswater.com

doi: 10.5004/dwt.2023.29277

285 (2023) 47–66
February

Diglycolamides as highly efficient carrier ligands for actinide transport in supported liquid membranes

Seraj A. Ansari*, Prasanta K. Mohapatra

Radiochemistry Division, Bhabha Atomic Research Centre, Mumbai-400085, India, emails: ansaris@barc.gov.in (S.A. Ansari), mpatra@barc.gov.in (P.K. Mohapatra)

Received 27 July 2022; Accepted 21 December 2022

ABSTRACT

The efficient separation of hazardous trivalent actinides from radioactive wastes remains a challenge to the global acceptance of nuclear power. With the dedicated efforts worldwide, diglycolamide (DGA) based ligands have been identified as the best extractants till today for the separation of trivalent actinides. Though the DGA-based ligands have been extensively studied in liquid–liquid extraction, in the last decade many interesting studies have appeared on supported liquid membrane-based separations utilizing these ligands. This article gives a comprehensive account of the studies that have been reported on DGA-based supported liquid membrane separation of actinides and lanthanides relevant to the back end of nuclear fuel cycle. Fundamentals of liquid membrane-based metal ion separations have been also discussed for designing the separation processes. Finally, a futuristic approach has been presented for the comprehensive investigation of DGA-based liquid membranes for their applications in radioactive waste management.

Keywords: Liquid membranes; Diglycolamide; Actinides; Separation; Waste management; Actinide partitioning

1. Introduction

Separations in the chemical industry do not need an introduction that often requires the product recovery and (or) purification. The terminology that is used to explain the separation phenomena varies widely depending on the subject and the readers. For a person dealing with chemistry and chemical engineering, the separation process is a mean of segregating a solution or a mixture of solids into their individual components. In few cases, the separation process may separate the mixture into pure constituents. In other cases, the process may separate a mixture of the desired product from the rest of the constituents. For separation, the process utilizes the differences in chemical or physical properties of its constituent to be separated such as size, shape, mass, density, chemical affinity, etc. Separation techniques are very commonly classified depending on the type of methodologies used. In most cases, multiple methods are utilized to get the desired separation as a single method that may be insufficient in getting the desired product.

Though the traditional separation methods such as solvent extraction, ion-exchange, and precipitation are being used extensively, these methods have certain merits and demerits [1,2]. Major limitations of the solvent extraction processes include phase disengagement limitations, third phase formation, generation of large volumes of secondary wastes, etc. Hence, there is a growing interest in developing suitable separation methods, such as supported liquid membrane (SLM) methods, which are considered to be environmentally benign due to the generation of very low amounts of secondary wastes in these methods [3,4]. Though the pressure-driven membrane separation methods are extremely popular for water purification and wastewater treatment, they are not selective, and therefore, selective separation of desired products requires better strategies. In this context,

* Corresponding author.

liquid membrane-based methods, for example, SLM containing selective carrier ligands, have received special attention from several researchers as evident by the growing publications in this area in the last few years (Fig. 1), though the number of publications was scattered before a decade.

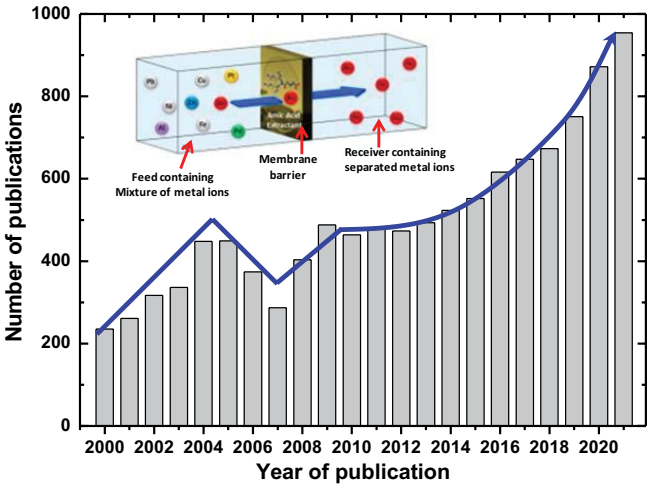

Fig. 1. Histogram chart showing the number of research papers reported since 2000. Source: Scopus. Keywords: Liquid membranes; Separation.

For nuclear industries desiring the close nuclear fuel cycle, the disposal of high-level waste (HLW) generated in spent fuel reprocessing is of great environmental concern [5,6]. To address this issue, the strategy of P&T (partitioning and transmutation) is being considered as an option that proposes the recovery of entire actinides (Am, Cm, Np, and Pu, also referred to as minor actinides) from HLW, and transmuting them into less hazardous nuclides for its safe disposal [6–11]. However, partitioning of minor actinides from HLW is a major challenge for separation scientists due to the presence of large concentrations of other metal ions in the waste. In this context, sustained efforts by the global researchers have identified diglycolamides (DGA) as one of the best extractants for actinide partitioning from HLW [12]. One of the DGA ligands, viz. *N,N,N′,N′*-tetra-*n*-octyl diglycolamide (TODGA, Fig. 2) has been most widely studied for actinide partitioning from HLW [7,13]. TODGA has been tested with genuine high active raffinate (generated from reprocessing of fast reactor spent fuels waste) at the European Union with highly encouraging results [14]. Till date, TODGA has been the most accepted extractant for actinide partitioning globally with some work also gaining importance with its branched chain homolog, TEHDGA (*N,N,N′,N′*-tetra-(2-ethyl-hexyl) diglycolamide). These ligands have also been studied in SLMs which are the focus of this article.

From a fundamental chemistry point of view, the DGA ligands are quite fascinating as they form chelates with the

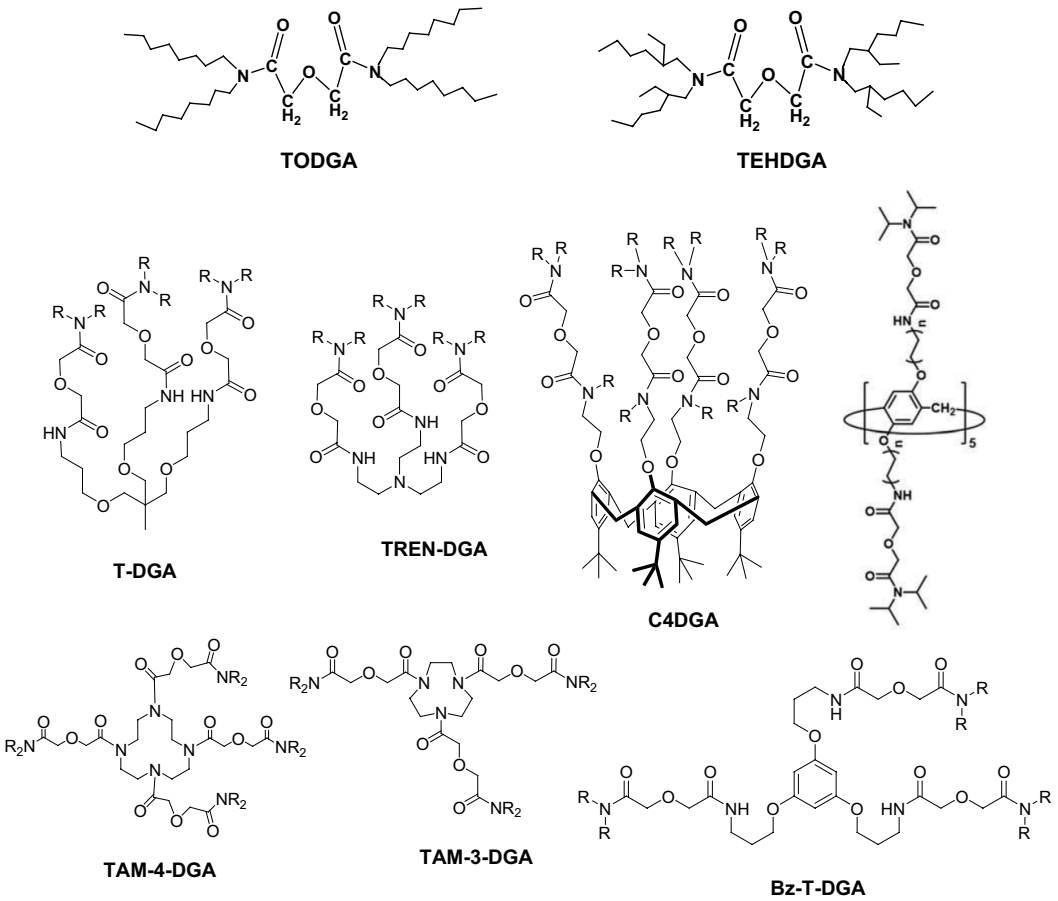

Fig. 2. Structures of diglycolamide (DGA) based ligands.

amidic and etheric 'O' atoms with varying complexation abilities. In view of the 'strategic' position of the central 'O' atom in DGA, binding with the two peripheral amidic 'O' atoms automatically brings the etheric 'O' atom close to the bonding distance. In view of these unique features, the chemistry of DGA ligands has been quite interesting as they show far better extraction ability for trivalent actinides. On the other hand, the extraction of hexavalent actinyl ions is relatively poor. Detailed studies carried out to understand such an unusual extraction behaviour suggested a peculiar mechanism. It was found that the extraction of metal ions with TODGA takes place via the formation of aggregates (reverse micelle), and the cavity size of the aggregates shows the highest selectivity for the metal ions having an ionic size of 100 ppm [15]. A detail SANS (small angle neutron scattering) study indicated that 3–4 TODGA molecules form a reverse micelle which eventually facilitated the extraction of the metal ions, thereby imparting a unique size selectivity akin to the crown ethers [16,17].

Keeping in mind the formation of aggregates in TODGA, a series of DGA ligands have been synthesized in the last few years, where multiple DGA groups are appended onto a suitable scaffold to mimic the aggregate structure of TODGA. Studies on such ligands gave much higher extraction efficiency of the ligands as compared to the bare TODGA ligand. A few examples of multiple DGA functionalize ligands are (Fig. 2): (i) 3 DGA moieties anchored onto a central C atom resulting in a tripodal framework (T-DGA), (ii) 3 DGA groups functionalized onto a central N atom (TREN-DGA), (iii) 4 DGA moieties attached to a calix [4] arene platform (C4DGA), (iv) 5 DGA functionalized pillarenes, (v) 3 or 4 DGA moieties functionalized onto a 9 or 12 membered tri (tetra) aza crown ether scaffold (TAM-3-DGA or TAM-4-DGA), and (vi) 3 DGA arms tethered to a benzene molecules at alternate 'C' atoms (Bz-T-DGA). Apart from these ligands, several DGA-functionalized dendrimers of zero, first, and second generations having as many as 8 DGA moieties on a diaminobutane platform were also synthesized and studied for actinide extraction [18,19]. Fundamental complexation studies with lanthanides (as surrogates for trivalent actinides) revealed that these multiple DGA ligands form much stronger complexes with the trivalent *f*-cations as compared to the simple DGA ligands such as TODGA or TEHDGA. Additionally, the multiple DGA functionalized ligands show higher selectivity for trivalent actinide ions over uranyl ions. These multiple-DGA ligands have also been studied in SLM separations, and have been discussed in this article.

Though the SLM-based separation methods have seen several applications, limited attention has been paid to these methods in the area of radionuclide separations [20,21]. This article aims to review and assimilate the scattered information at one place on the separation of actinides and lanthanides (radionuclides) using SLMs. Since there are several ligands that have been studied for the separation of actinides and lanthanides [22–24], this article will focus only on the work that has been reported using DGA ligands. Furthermore, the fundamentals of SLM-based separation have been discussed in detail for understanding the selective transport of metal ions (carrier-assisted transport phenomenon). Since the transport phenomenon in liquid membranes is fundamentally associated with the liquid–liquid extraction processes at the membrane interfaces, a brief outline of this aspect is also studied.

2. Liquid–liquid extraction phenomenon in membranes

Liquid–liquid extraction is a separation method that works on the principle of solute distribution. The method utilizes the difference in the solubility of a species or a compound or a solute in two immiscible liquids. For example, when a metal ion (M^{n+}) distributes itself between the aqueous phase and a water-immiscible organic liquid, its distribution coefficient (K_d) is given as:

$$K_d = \frac{\left[M^{n+}\right]_{(org)}}{\left[M^{n+}\right]_{(aq)}} \quad (1)$$

where the subscripts '(org.)' and '(aq.)' refer to the species in the organic and the aqueous phases, respectively. Since the metal ions are hydrophilic in nature, they tend to remain in the aqueous phase due to ion–dipole interaction, and they will not move to the organic phase unless the charge on the metal ion is neutralized. To neutralize the charge on the metal ion and to make it hydrophobic, a suitable ligand is generally added in the organic phase which forms complex with the metal ion and makes it hydrophobic facilitating its movement from the aqueous phase to the organic phase. The fundamental laws that govern the separation of metal ions in the liquid–liquid extraction are: (i) the chemical reaction between the metal ions and the ligand at the aqueous-organic interface, (ii) the kinetics of the chemical reaction at the organic-aqueous interface, and (iii) the fluid mechanics and mass transfer of the metal/ligand complex (or any species to be separated) from aqueous to organic phase. The fundamental principles that control the metal ion separation in liquid–liquid extraction are identical to the major steps in liquid membrane separation. The additional principle that controls the separation in the liquid membrane is the diffusion of species inside the liquid membrane explained below.

3. How membrane separation processes work?

In the process of membrane separation, two aqueous phases are physically separated by a membrane barrier. Out of the two phases, one is known as feed which contains the mixture of species to be separated, and the other is the receiver where the separated species get collected. In membrane separation processes, only the targeted species from the feed side are allowed to pass through the membrane, and the rest of the species are retained in the feed. Broadly, the membrane separation processes are fundamentally described by one of the following principles: (i) size exclusion, (ii) Donnan exclusion, and (iii) diffusion. In any of these principles, the driving force for transporting the species from the feed side to the receiver side of the membrane is provided by (i) the trans-membrane hydrostatic pressure, (ii) osmotic pressure, and (iii) the concentration gradient across the membrane.

3.1. Separation based on size exclusion principle

As the name specifies, these membrane processes work on the size exclusion principle [25], where the molecules of larger size than the membrane pores are retained on one side of the membrane, and the smaller size molecules are allowed to pass through it. These membrane processes are very often referred to as filtration process. Based on the pore size of the filters, the processes can be further sub-classified as microfiltration, ultrafiltration, reverse osmosis, or nanofiltration. The driving force for most of these filtration processes is the pressure that is applied across the membrane. Different types of such filtration processes are shown in Fig. 3.

3.2. Separation based on Donnan exclusion principle

The Donnan phenomenon is commonly referred to as "Donnan Law" or "Donnan Equilibrium" or "Gibbs–Donnan Equilibrium". This phenomenon is observed in the solutions containing large size positively or negatively charged species that is retained by the semi-permeable membrane, but their smaller counter ions are allowed to pass through it. Because of this effect, an uneven electrical charge is created across the membrane surface. In this phenomenon, an electric potential is generated on both sides of the membrane, known as Donnan potential. One of the best examples of Donnan effect is observed in the blood circulatory system, where bigger size protein molecules in the plasma (which are anionic in nature) are retained by the blood capillary walls, but other small cations like K^+ and Na^+ can freely pass through the wall [26]. The other example is observed in the dye industry, where small sodium counter ions are separated from the large molecules of water-soluble dyes (water-soluble dyes are basically sodium salts) [27]. For separating sodium from the dyes, the dye solution and pure water phases are separated through a semi-permeable membrane. An electrical potential is applied across the membrane which causes the sodium ion penetrates through the semi-permeable membrane from the dye solution to the other side of the membrane, but the large dye anions are retained in the solution. This causes the excess of negative charge in the feed solution and excess of positive charge in the receiver phase. To maintain electro-neutrality, water molecules are split in the feed solution; H^+ ions remain associated with the dye anion, and OH- ions migrate with the Na^+ ions into the receiver phase. Therefore, a highly concentrated dye in the acid form gets separated in one compartment and sodium hydroxide in the other compartment.

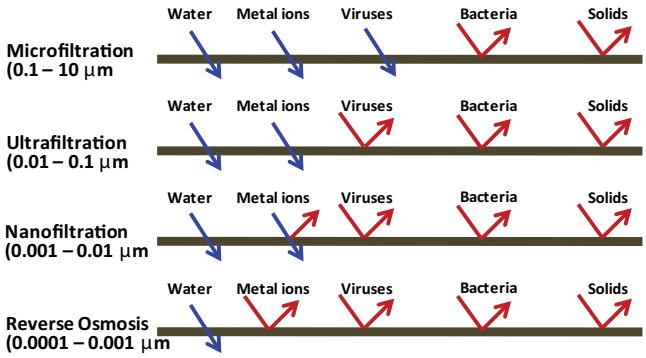

Fig. 3. Schematic representation of membrane filtration processes.

3.3. Separation based on the diffusion principle

In the case of membrane working on diffusion principle, the species are first concentrated on one side of the membrane surface either by physical sorption or by complexation with a ligand. Due to this, a concentration gradient of the species arises across the membrane. As a consequence, there will be diffusion of the species from the higher concentration side of the membrane to the other side of the membrane leading to its separation. SLM-based separations are the best example of diffusion-controlled process which is the interest of this article.

4. How liquid membranes are different?

Pressure-driven membrane processes, such as reverse osmosis, nanofiltration, ultrafiltration, and microfiltration, are the workhorse of industrial plants working for the treatment of wastewater. As these processes work on the principle of size exclusion, they show poor selectivity for metal ions due to their similar ionic sizes. To impart selectivity in such processes, a metal ion selective bulky ligand is added to complex the metal ions which are then retained by the membrane, and thus separated from the host of metal ions. A few examples of such separation processes are micellar-enhanced ultrafiltration, which is quite useful in wastewater treatment [28,29], and complexation–ultrafiltration [30,31]. These methods will not be discussed here as they are outside the scope of this article. On the other hand, very high selectivity is obtained in liquid membrane processes, particularly for metal ion separation, due to the utilization of highly metal ion selective ligands [32]. In this method, a water-immiscible ligand solution (organic phase) is used as a liquid membrane to physically separate the two aqueous solutions (feed and receiver solutions). On the feed side, the ligand selectively complexes with the target metal, and then the metal-ligand complex travels from the feed side across the membrane to the receiver side. Such transport processes are, therefore, referred to as "carrier-mediated transport" or "carrier-facilitated transport" processes.

Thus, a liquid membrane is basically a water-immiscible organic layer, which acts as a barrier between the feed and the receiver solution. Based on the type of liquid used as the barrier, liquid membranes are further classified as (i) bulk liquid membrane (BLM), (ii) emulsion liquid membrane (ELM), and (iii) supported liquid membrane (SLM). Fig. 4 gives a general representation of various types of liquid membranes. In BLM, the liquid membrane is a stirred organic phase that separates the feed and the receiver phase, while a dispersed receiver phase (entrapped in oil droplets) in the feed solution is used in ELM. In SLM on the other hand, a water-immiscible organic phase is immobilized in the pores of an inert microporous polymeric membrane that separates the feed and the receiver phases. When the membrane support is a flat sheet, the method is known as flat sheet SLM, while the

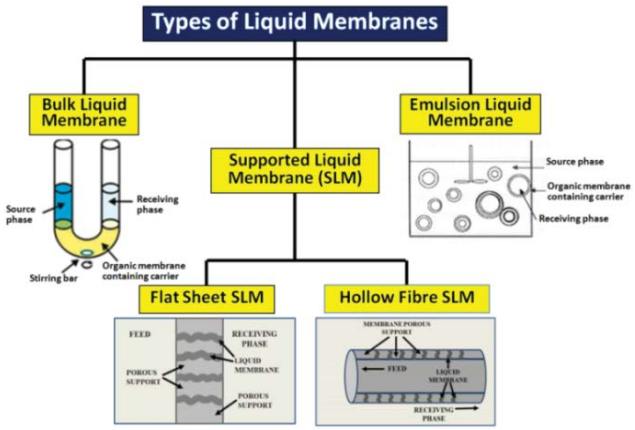

Fig. 4. Different types of liquid membranes. Reproduced with permission from Ansari and Mohapatra [20].

name hollow fibre SLM is given when a bunch of hollow fibres are used as the membrane support.

5. Transport mechanism in SLMs

As mentioned earlier, the fundamental principle that relates to the transport of given species in a liquid membrane is the 'carrier facilitated transport' since the carrier ligand picks-up the metal ion from one side of the membrane and carries it to the other side. Fig. 5 gives a typical representation of the metal ion transport by a neutral carrier ligand. In the 'carrier facilitated transport' process, four basic steps are involved that governs the overall transport efficiency. *Step I*: diffusion of the metal ion from bulk feed solution to the membrane surface to form a metal-ligand complex (ML) on the membrane surface. *Step II*: diffusion of the ML complex from feed to receiver side within the membrane through diffusion process. *Step III*: dissociation of the ML complex at the membrane surface on the receiver side to release the metal ions in the receiver solution, and ligand in the membrane phase. *Step VI*: back diffusion of the free ligand within the membrane from the receiver side to the feed side. These four steps are repeated till the entire metal ion is transported from the feed to the receiver side.

In order to initiate the metal ion transport, the equilibrium reaction shown in Fig. 5 must be favored on the feed side of the membrane, and the reverse must be the case on the strip side. Therefore, it is essential to maintain the feed condition such that the ML complex is instantaneously formed at the feed-membrane interface. If the entire ligand gets complexed with the metal ion at the feed-membrane surface, the free ligand concentration on this surface will be very low. At the same time, it is essential to maintain the receiver phase condition such that the ML complex is instantaneously dissociated at the strip-membrane interface. If the entire ML complex gets dissociated at the strip-membrane surface, the free ligand concentration on this surface will be very high. Due to the higher concentration of ML complex on the feed-membrane surface, and free ligands at the strip-membrane surface, there will be positive concentration gradients for ML complex at the feed side, and free ligands at the strip side of the membrane surface. Consequently, the

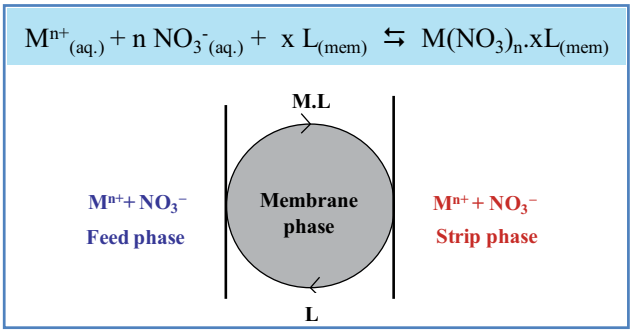

Fig. 5. Schematic representation of metal ion transport by a neutral ligand.

ML complex will always diffuse from the feed to the strip side, and free ligands from the strip to the feed side. This diffusion process can be well explained with the help of Wilke–Chang empirical equation [33].

$$D_o = 7.4\times10^{-8}\left(\frac{\chi^{0.5}M^{0.5}T}{\eta V_m^{0.6}}\right) \quad (2)$$

where D_o is the diffusion coefficient of the species (metal-ligand complex or bare ligand), M, χ and η are the molecular weight, solvent association parameter, and viscosity of the solvent, respectively, V_m is the molar volume of the carrier and T is the temperature. As V_m of the ML complex will be higher than that of the free ligand, the back diffusion of the free ligand from the strip to the feed side will be faster. Consequently, the free ligand will be available every time for complexing with a metal ion.

6. Transport equations in SLMs

Various transport equations in the liquid membranes are derived by taking into account of the metal ion concentrations at the feed and strip side of the membrane. As depicted in Fig. 5, derivation of different transport equations is possible only with the specific knowledge of the following steps: (i) diffusion of the metal ion in the aqueous boundary layer on the feed side, (ii) forward equilibrium reaction taking place on the feed side of the membrane surface, (iii) diffusion of the metal-carrier complex within the membrane phase, and (iv) backward equilibrium reaction taking place at the strip side-membrane surface. The basic mathematical equations for metal ion transport in liquid membranes have been derived by incorporating a few assumptions [32]. It is assumed that the chemical reactions between the metal ions and the ligand at both sides of the membrane surfaces are very fast as compared to the diffusion of the species. It implies that the chemical reaction equilibrium taking place on the membrane surfaces is not the rate-determining step, but the diffusion of the species inside the membrane phase will control the transport rate. Therefore, the basic transport equation in the liquid membrane is governed by different diffusion laws. According to the Fick's first law of diffusion, the flux (J) of the permeating species in the membrane phase is given as [32]:

$$J = -\frac{\partial C}{\partial t} \times \frac{V}{A} \text{ (mg/cm}^2\text{/s)} \quad (3)$$

where V = volume of the feed solution, C = concentration of the metal ion, and A = surface area of the membrane. As the term J in Eq. (3) is concentration dependent, the term "permeability coefficient (P, cm/s)" is commonly used to relate the membrane efficiency, which is independent of the concentration term. The quantity P is derived by dividing the term J with the concentration. Therefore, the flux, J, is given as:

$$J = P \times C \quad (4)$$

Eqs. (3) and (4) can be equated as:

$$P \times C = -\frac{\partial C}{\partial t} \times \frac{V}{A} \quad (5)$$

$$\int \frac{\partial C}{C} = -P\left(\frac{A}{V}\right)\int \partial t \quad (6)$$

$$\ln\left(\frac{C_t}{C_o}\right) = -P\left(\frac{A}{V}\right)t \quad (7)$$

Eq. (7) is used to determine the permeability coefficient of any permeating species experimentally. The permeability coefficient quantifies the transport of a given species, and hence, is considered as one of the primary parameters defining the transport efficiency. Here, the ratio of the concentration of the metal ion at time t to its initial concentration in the feed is plotted against the time. The value of P is then calculated from the slope of the linear fit of the plot. By using the known volume of feed solution (V) and known membrane surface area (A), the value of P is calculated from the slope.

As mentioned earlier, the diffusion of the ML complex in the membrane phase (D_o) is indeed the rate-determining step, which governs the overall flux of the diffusing species [32]. The flux, J, is correlated with D_o as:

$$J = -D_o \frac{\partial C}{\partial x} \quad (8)$$

where x is the diffusion path length, which is the thickness of the membrane in the present case. For metal ion transport, Eq. (8) can be modified as:

$$J = -D_o \times \frac{\left[\text{ML}\right]_f - \left[\text{ML}\right]_r}{d_o} \quad (9)$$

where $[ML]_f$ = concentration of the ML complex at the feed-membrane side, $[ML]_r$ = concentration of the ML complex at the strip-membrane side and d_o = thickness of the membrane. In SLM, a membrane filter is impregnated with a ligand solution in a suitable solvent which acts as the liquid membrane. Based on ligand properties, the feed condition is maintained such that instant metal/ligand complexation occurs at the membrane surface. Similarly, a non-favored condition is maintained in the strip solution so that the ML complex is dissociated instantly. Consequently, the term $[ML]_f$ will always be more than the $[ML]_r$ in Eq. (9), and ∂C will be always positive to drive the metal ion transport.

The factor affecting the diffusion coefficient of the species in the membrane phase (D_o) is represented by the following Einstein–Stoke equation:

$$D_o = \frac{k \times T}{6\pi\eta r} \quad (10)$$

where k = Boltzmann constant, T = absolute temperature, η = viscosity of the medium, and r = radius of the diffusing species. In order to achieve higher D_o values, one has to use low-viscosity solvents in the liquid membranes. In simple words, to achieve efficient transport of liquid membranes, the ligands used should be dissolved in the lowest possible viscous solvent. Additionally, the membrane thickness should be as low as possible to get higher D_o values. In SLM, since the thickness of the membrane is decided by the thickness of the membrane support, optimum D_o values can be achieved by choosing the membrane support having minimum thickness with good mechanical stability.

From the above discussion, it can be concluded that for an optimum transport of metal ions in SLMs, one should control the following parameters: (i) the ligand should be selected such that it forms a reversible complex (easy complex formation and dissociation) with the target metal ion, (ii) the ligand solution (membrane phase containing ligand) should have reasonably low viscosity, (iii) the distribution ratio of the target metal ion should be large under the given aqueous feed condition, and should be very low under given receiver phase condition, and (iv) effective surface area of the membrane should be high with minimum possible thickness. By careful optimization of these parameters, efficient transport of the metal ions can be achieved in SLMs.

7. DGA ligands in SLMs

The literature survey points out that one of the DGA ligands, viz. TODGA, has been the most widely studied extractant for actinide partitioning in liquid–liquid extraction [7,12,13]. Scores of reports are also available, where TODGA has been studied in liquid membranes [34–40]. In addition to TODGA, which has a linear octyl chain, a branched alkyl chain ligand, viz. TEHDGA has also been studied for the separation of actinides in liquid membranes [41–45]. Table 1 summarizes a series of SLM studies that have been performed with DGA-based ligands. A brief discussion of these studies is given in this article.

7.1. SLM studies with linear chain DGA (TODGA)

Since their first report on the use of TODGA for actinide ion extraction in 2001 by Sasaki et al. [46], the group studied various other aspects of the extraction of lanthanide/actinide ions by TODGA [46–48]. The authors of this article also were quite active in studying the extraction behavior

of actinides using TODGA and were probably the first to investigate the performance of TODGA in SLM [34]. With 0.1 M TODGA in *n*-dodecane as the carrier ligand impregnated inside the pores of PTFE membrane filters, quantitative (>99.9%) transport of Am^{3+} was noted within 4 h at 20 mL scale. Transport was not affected by changing the feed acidity between 1–5 M HNO_3 with distilled water as the receiver phase. However, the transport was suppressed at 6 M HNO_3 due to the large co-transport of acid from the feed to the receiver phase (Table 2). Formation of TODGA×HNO_3 complexes have been reported by many authors at lower acidities [49] which changes to TODGA×$(HNO_3)_2$ at higher aqueous phase acidity [50]. Apparently at 6 M HNO_3, the TODGA×$(HNO_3)_2$ species facilitates a large amount of acid transport thereby affecting the metal ion transport. The transport rates were influenced by the TODGA concentration, and aqueous nitrate ions concentration. Interestingly, sodium nitrate concentration in the feed (0.5–3 M at 0.01 M HNO_3) was less effective for the transport of Am^{3+} as compared to the nitric acid concentration. In an experiment carried out at a constant nitrate ion concentration (3 M), the increase in the metal ion permeability was much steeper at a lower nitric acid concentration. At higher nitric acid concentrations, a plateau was observed indicating the decreasing influence on metal ion transport (Fig. 6a). This behaviour resembled the distribution ratio (*D*) data obtained in liquid–liquid extraction (Fig. 6b), suggesting the importance of the equilibrium operating at the feed–membrane interface. Similar to the results obtained during the solvent extraction, the presence of $NaNO_3$ (at 0.01 M H^+ ions) was found to enhance the Am^{3+} pertraction, though not as effectively as seen with pure HNO_3. However, the profile of *P* vs. [$NaNO_3$] (Fig. 6c) resembles that of D_{Am} vs. [$NaNO_3$] (Fig. 6d), suggesting the extraction process is indeed a key step in the transport process.

Fig. 7 represents the transport profile of actinides, lanthanides, and some of the fission products by TODGA-SLM. The transport of tri- and tetravalent actinides was higher than those of the hexavalent actinides [35]. It is well accepted that the trivalent actinides form a stronger complex with TODGA than the hexavalent actinyl ions [12]. Consequently, Am^{3+} gives a better transport profile than UO_2^{2+}. The transport profile of Eu^{3+} followed the trivalent actinides. It was noted that the Am^{3+} transport was not affected by the presence of large concentration of uranium (20 g/L) or Fe (6 g/L) [35]. However, its transport was significantly reduced in the presence of non-distinguishable lanthanides. In the presence of ~0.6 g/L lanthanides in the feed, >15 h was necessary for the quantitative transport of Am^{3+}, which could be completed within 4 h in the absence of lanthanides. The transport of Pu^{4+} was at par with that of Am^{3+}, indicating that the former can be recovered along with the trivalent actinides and lanthanides by TODGA-SLM. The transports of fission and structural elements were >99.9% Zr^{4+}, ~8% Ru^{3+}, ~85% Sr^{2+}, and ~56% Pd^{2+} in 5 h [35,36]. However, the addition of 0.4 M oxalic acid in the feed suppressed the transport of Zr^{4+} significantly without affecting the transport of Am^{3+} (Fig. 8). Negligible transport of Mo and Cs was observed while Tc was transported in a significant quantity.

Table 2
Permeation data of Am^{3+} with TODGA-SLM. Membrane: 0.45 mm PTFE; carrier: 0.1 M TODGA in *n*-dodecane; receiver: distilled water [34]

Feed acidity, [HNO_3], M	$P \times 10^3$ (cm/s)	% Transport (after 4 h)	Strip phase acidity (after 4 h), M
1.0	2.1 ± 0.3	99.8	0.02
2.0	3.8 ± 0.7	101.2	0.05
3.0	3.7 ± 0.4	100.2	0.07
4.5	3.1 ± 0.2	100.0	0.10
6.0	2.2 ± 0.1	96.9	0.13

Table 1
Summary of SLM studies performed for actinide separation using DGA-based ligands

Ligand	Solvent	Transport data after 3 h	References
0.1 M TODGA	*n*-dodecane	Feed: 3 M HNO_3, strip: 0.1 M oxalic acid, Th^{4+} = 75%, Pu^{4+} = 85%	[37,51]
0.1 M TPDGA	*n*-dodecane	Feed: 3 M HNO_3, strip: 0.1 M HNO_3, Am^{3+} = 90%	[40]
0.1 M THDGA	*n*-dodecane	Feed: 3 M HNO_3, strip: 0.1 M HNO_3, Am^{3+} = 49%	[40]
0.1 M TODGA	*n*-dodecane	Feed: 3 M HNO_3, strip: 0.1 M HNO_3, Am^{3+} = 93%	[40]
0.1 M TDDGA	*n*-dodecane	Feed: 3 M HNO_3, strip: 0.1 M HNO_3, Am^{3+} = 72%	[40]
0.1 M TEHDGA	*n*-dodecane	Feed: 3 M HNO_3, strip: 0.1 M HNO_3, Am^{3+} = 88%	[40]
0.2 M TEHDGA	*n*-dodecane	Feed: 3 M HNO_3, strip: 0.1 M HNO_3, Am^{3+} = 99%	[41]
4 mM T-DGA	10% *iso*-decanol/dodecane	Feed: 3 M HNO_3, strip: 0.01 M EDTA, Am^{3+} = 98%	[69]
4 mM DGA-TREN	5% *iso*-decanol/dodecane	Feed: 3 M HNO_3, strip: 0.01 M HNO_3, Am^{3+} = 40%	[73]
1 mM Bz-T-DGA	5% *iso*-decanol/dodecane	Feed: 3 M HNO_3, strip: 0.01 M HNO_3, Am^{3+} = 45% (L_1), 10% (L_2), 70% (L_3)	[78]
C4DGA, L_1, L_3 = 1 mM, L_2 = 10 mM	5% *iso*-decanol/dodecane	Feed: 3 M HNO_3, strip: 0.01 M EDTA, Am^{3+} = 28% (L_1), 77% (L_2), 75% (L_3)	[86]
1 mM DGA-dendrimers	5% *iso*-decanol/dodecane	Feed: 3 M HNO_3, strip: 0.01 M HNO_3, Am^{3+} = <5% (0^{th}_{Gen}), 62% (I^{st}_{Gen}), 78% (2^{nd}_{Gen})	[87]

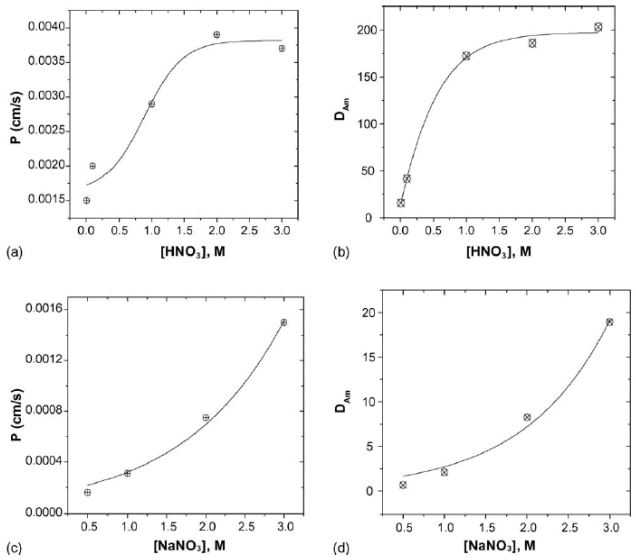

Fig. 6. (a) Transport, (b) extraction data of Am^{3+} with increasing HNO_3 concentration at 3 M $NaNO_3$, (c) transport, and (d) extraction data of Am^{3+} as a function of $NaNO_3$ concentration at pH 2. Reproduced with permission from the study of Ansari et al. [34].

Panja et al. [37] extensively studied the transport of tetravalent actinides, viz. Th^{4+} [51] and Pu^{4+} in flat sheet TODGA-SLM. Interestingly, it was found that the transport of Th^{4+} at the tracer level from 3 M HNO_3 feed to water (receiver phase) was only about 85% in 6 h, though the D_{Th} value was 1.58×10^4 [51]. The D_{Th} value was much higher than those reported for the trivalent actinides and lanthanides (D values = 300–600), but the Th^{4+} transport was only about 85% as compared to the cent percentage transport of trivalent lanthanides and actinides. The transport of Th^{4+} was only marginally improved to about 90% when oxalic acid was employed as the strip phase. On the other hand, its transport declined drastically and reached a saturation value of 30% in the presence of 5 g/L Th. On the other hand, the transport of Pu^{4+} (at tracer scale) from 3 M HNO_3 feed into 0.1 M oxalic acid was about 98% in 6 h [37]. In this work, the authors reported the $D_{Pu(IV)}$ value of 10.59, which was magnitudes of order lower than the D_{Th} values. However, the lower transport of Th^{4+} as compared to Pu^{4+} under identical conditions could not be explained based on the distribution values. The authors also confirmed the valency of Pu as Pu^{4+} by optical spectroscopy even after 24 h, which ruled out any changes in the oxidation state of Pu^{4+} during the experiment. In another study [38], it was shown that Pu^{3+} transport was 94% in 3 h vis-à-vis 99% Am^{3+} and 67% Th^{4+} under identical experimental conditions. On the other hand, the transport of hexavalent actinyl ions, viz. UO_2^{2+} and PuO_2^{2+}, was between 60% and 70% in 6 h, which is expected from low distribution values of these actinyl ions with TODGA [52]. The difference in the transport profiles of Am^{3+}, Pu^{4+}, Th^{4+} and UO_2^{2+} was not only dependent on their D values, but also on the composition of their transported species, which were $[Am(TODGA)_3(NO_3)_3]$, $[Pu(TODGA)_2(NO_3)_4]$, $[Th(TODGA)_2(NO_3)_2]$ and $[UO_2(TODGA)_2(NO_3)_2]$, respectively.

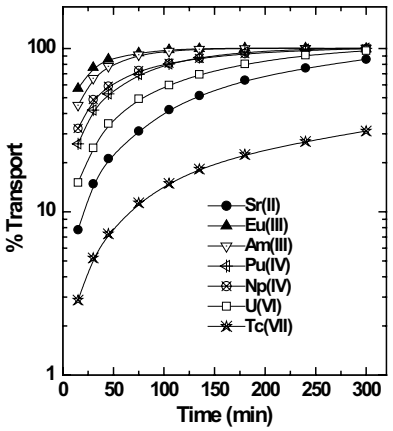

Fig. 7. Transport of metal ions by TODGA-SLM by TODGA-SLM. Feed: 3 M HNO_3; receiver: distilled water. Reproduced with permission from the study of Ansari et al. [35].

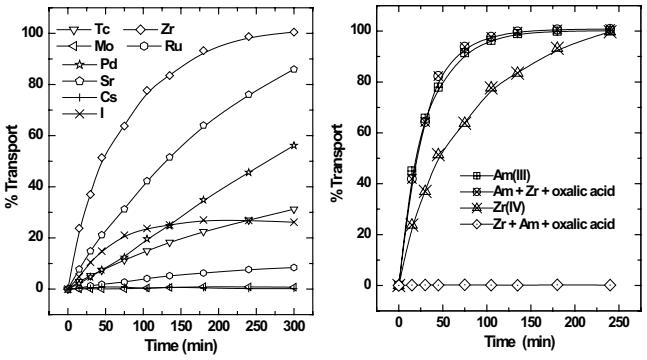

Fig. 8. Transport of metal ions by TODGA-SLM; Feed: 3 M HNO_3; receiver: distilled water. Reproduced with permission from the study of Ansari et al.[36].

7.2. SLM studies with branched chain DGA (TEHDGA)

SLM studies with branched alkyl DGA, viz. TEHDGA, has been exclusively reported from Bhabha Atomic Research Centre, India [41–45]. With 0.2 M TEHDGA in *n*-dodecane as the carrier, Am^{3+} transport was quantitative in 3 h from 3 M HNO_3 feed [41]. The use of a two times higher concentration of TEHDGA (0.2 M) as compared to TODGA (0.1 M) in this work was justified in view of the lower extraction efficiency of the branched alkyl chain DGA [53]. The membrane stability was excellent as monitored over a period of 22 d of continuous use. The Am^{3+} diffusion coefficient through the TEHDGA membrane was experimentally obtained as 1.27×10^{-6} cm^2/s, which was an excellent match with the value of 1.22×10^{-6} cm^2/s calculated theoretically. However, the selectivity for Am^{3+} over other metal ions present in the acidic feed (3 M HNO_3) solution was found to be poor (Fig. 9). Interestingly, the authors also reported about 8% transport of Cs^+, but the transport of UO_2^{2+} and Pu^{4+} was less than 3% under identical conditions monitored after 4 h of the transport experiment [52]. In another study, the same authors reported similar transport behaviour of Eu^{3+} with 0.2 M TEHDGA [43]. However, despite higher D_{Eu} than D_{Am}, the permeability

coefficient of the former metal ion with TEHDGA was reported to be about 4 times lower than the later, the reason for which could not be explained. This could be possibly due to the difference in the nature of diffusing species though no study to this effect was taken up by the authors. An interesting observation was noted while investigating the effect of temperature on the transport of Eu^{3+} by TEHDGA-SLM [43]. Though the extraction of trivalent *f*-cation with TEHDGA and TODGA both are exothermic in nature [53], the transport of Eu^{3+} was found to increase with temperature. This feature may be ascribed to the lowering in the viscosity of the membrane phase at elevated temperatures which favoured the diffusion of the complex in the membrane phase.

DGA ligands are known to form the third phase in solvent extraction studies [47,54–56]. The problem of third phase formation may create a problem in SLM if the metal/ligand complex aggregates at the membrane surface, and cause choking of the membrane pores. The problem of third-phase formation is easily overcome by increasing the overall solvent polarity with the help of phase modifiers [57,58]. In the case of DGA ligands such as TODGA and TEHDGA, the use of 5%–30% *iso*-decanol along with *n*-dodecane has been recommended as the phase modifier which could avoid the formation of third phase formation [59,60]. Panja et al [43], systematically investigated the effect of *iso*-decanol along with 0.2 M TEHDGA on the transport of Eu^{3+}. It was observed that while in the absence of *iso*-decanol, ~95% Eu^{3+} got transported in 5 h, its transport decreased continuously after the addition of *iso*-decanol (Fig. 10), and only ~72% Eu^{3+} transport was recorded in the presence of 40% *iso*-decanol. Authors also reported a similar effect on the transport of UO_2^{2+} by TEHDGA-SLM [42], where the transport decreased from 81% without phase modifier to 64% when 40% *iso*-decanol was used as the phase modifier. Authors attributed this decrease in the transport to the increased polarity of the solvent resulting in poor extraction, and hence, lower transport. However, the authors did not investigate the acid co-transport in the presence of *iso*-decanol which has a significant role in acid extraction. It is expected that the presence of *iso*-decanol will enhance the strip phase acidity, which in turn would suppress the stripping efficacy of the receiver phase, and hence, would reduce the overall transport. This feature is well documented where it has been shown that the complete stripping of Nd^{3+} from the loaded TODGA phase containing 30% *iso*-decanol requires more than 6 stages, whereas the stripping is complete in just two stages if 5% *iso*-decanol is used [59].

In another work, a detail investigation on the transport of UO_2^{2+} and Pu^{4+} was reported with 0.2 M TEHDGA in 30% *iso*-decanol + 70% *n*-dodecane [45]. It was shown that the nature of mineral acids did affect the transport of actinyl ions due to change in the metal/ligand complex species that was transported across the membrane. When different mineral acids (3 M) were used as the feed solution, the transport of actinyl ions followed the trend HNO_3 >> HCl ~ $HClO_4$ [45]. The transport rate did not change much when the respective sodium salts were used in the feed, suggesting that the transport of acid was not much, and it was not affecting the transport rate. Compared to UO_2^{2+}, Pu^{4+} transport was significantly lower as the latter was only about 50% in 5 h as compared to about 80% transport of the former under identical experimental conditions. This trend may be explained based on the ionic potential consideration of the two actinyl ions. The transport of UO_2^{2+} was lower with TEHDGA as compared to those seen with TODGA, which is opposite to the distribution ratio values reported by the two ligands. The $D_{U(VI)}$ value at 3 M HNO_3 with TODGA is 4.99 [52] vis-a-vis 7.63 with TEHDGA [44] under an identical feed acidity. The stoichiometry of the extracted complex was also identical for both the ligands, where mono-solvated species were extracted, viz. $UO_2(NO_3)_2 \times L$, where L = TODGA or TEHDGA. On the other hand, TODGA and TEHDGA both gave similar transport for Pu^{4+}. Nonetheless, the important conclusion that can be drawn from these observations are that the transport of trivalent and tetravalent actinides is highly efficient with both the DGA ligands when compared with the hexavalent actinyl ions, primarily due to the low affinity of the actinyl ions.

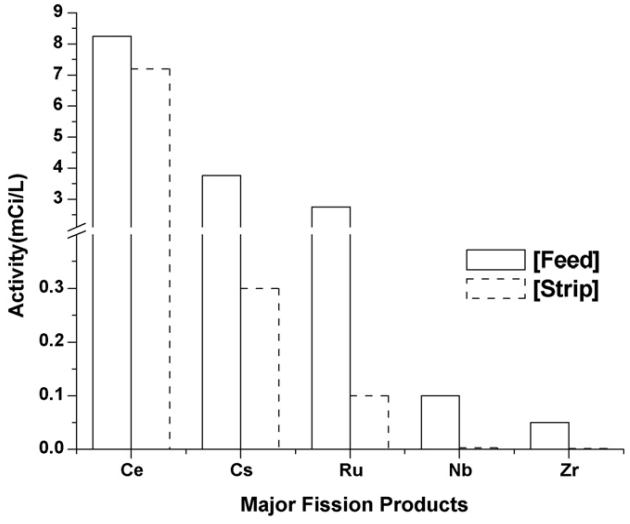

Fig. 9. Transport of fission products across 0.1 M TEHDGA-SLM. Feed: 3 M HNO_3; strippant: 0.1 M HNO_3. Reproduced with permission from the study of Panja et al.[52].

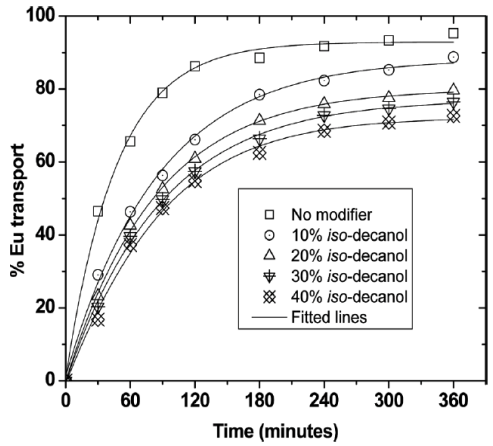

Fig. 10. Effect of phase modifier on transport of Eu^{3+} by TEHDGA-SLM. Feed phase: 3 M HNO_3, Receiver phase: 0.01 M HNO_3. Reproduced with permission from the study of Panja et al. [43].

Panja et al [40] investigated the effect of alkyl chain of DGA on the transport of Am^{3+}, Eu^{3+}, and Sr^{2+} in SLM. The transport data and the physical properties of the ligands solutions are summarized in Table 3. One may expect a similar transport profile of Am^{3+} and Eu^{3+} with these ligands as reflected in their distribution ratio. It is worth mentioning that the extraction of trivalent actinides and lanthanides decreases steadily with increasing the alkyl chain length from *n*-pentyl DGA (TPDGA) to *n*-decyl DGA (TDDGA) [46]. However, poor extraction and complexation constant with the branched alkyl chain derivative, viz. TEHDGA, was reported due to steric hindrances expected during the complexation process [53]. Similar decreasing trends have been also evident from the complexation constants of Nd^{3+} with varying alkyl chain derivatives of DGA [61,62]. A similar effect was also seen in the complexation of uranium by DGA ligands [63,64]. In the transport studies, however, no pattern in the transport profiles of either Am^{3+} or Eu^{3+} was observed (Table 3). For Am^{3+}, the transport profile followed the order: TODGA > TPDGA ~ TEHDGA > TDDGA > THDGA. Another observation in the transport profile that could not be explained was the lower transport of Eu^{3+} as compared to those of Am^{3+} with all the ligands, though the extraction of the former metal ion with DGAs was generally higher than those seen with the later one.

7.3. Transport of Sr^{2+} with DGA-SLM

Fig. 11a shows the transport profile of Sr^{2+} with 0.1 M DGA ligands dissolved in *n*-dodecane [40]. Maximum transport was observed for THDGA (tetra-hexyl derivative of DGA) and minimum transport was seen for TDDGA (*n*-decyl derivative). Nonetheless, higher than 25% co-transport of Sr^{2+} with any of the DGA ligands indicated poor decontamination of the Am^{3+}. In order to suppress the transport of Sr^{2+}, authors took the help of literature which indicated that the presence of 30% *iso*-decanol in the TODGA phase suppressed the extraction of Sr^{2+} significantly. As evidenced from Fig. 11b, the presence of *iso*-decanol drastically reduced the Sr^{2+} transport for TODGA, TEHDGA, and TDDGA. However, the Sr^{2+} transport rates (in 6 h) were still quite significant for THDGA (~38%), and TPDGA (~50%) with 30% *iso*-decanol, suggesting that TEHDGA and TDDGA were found to be better for decontamination of Sr^{2+}.

7.4. SLM studies with multiple DGA ligands

In the past few years, a series of DGA ligands have been synthesized where multiple DGA groups are appended onto a suitable scaffold [65–87]. Studies on such ligands gave much higher extraction efficiency of the ligands as compared to the simple DGA molecules such as TODGA. A few

Table 3
Transport data of Am^{3+} and Eu^{3+} with DGA Ligands. Ligand: 0.1 M in *n*-dodecane; feed: 3 M HNO_3; strip: 0.01 M HNO_3; membrane: 0.2 mM PTFE

Ligand (0.1 M)	Viscosity (mPa·s)	Density (g/L)	Am^{3+} Transport [40]		Eu^{3+} Transport [39]	
			$P \times 10^3$ (cm/s)	%*T* in 3 h	$P \times 10^3$ (cm/s)	%*T* in 3 h
TPDGA[a]	1.315	0.736	2.32	90.0	–	71.2
THDGA	1.621	0.745	1.52	49.2	1.56	28.0
TODGA	1.641	0.758	3.14	93.4	2.96	66.0
TEHDGA	1.639	0.757	1.96	87.8	2.47	54.9
TDDGA	2.415	0.787	1.02	72.4	4.37	64.3

[a]Data with 30% *iso*-decanol as phase modifier.

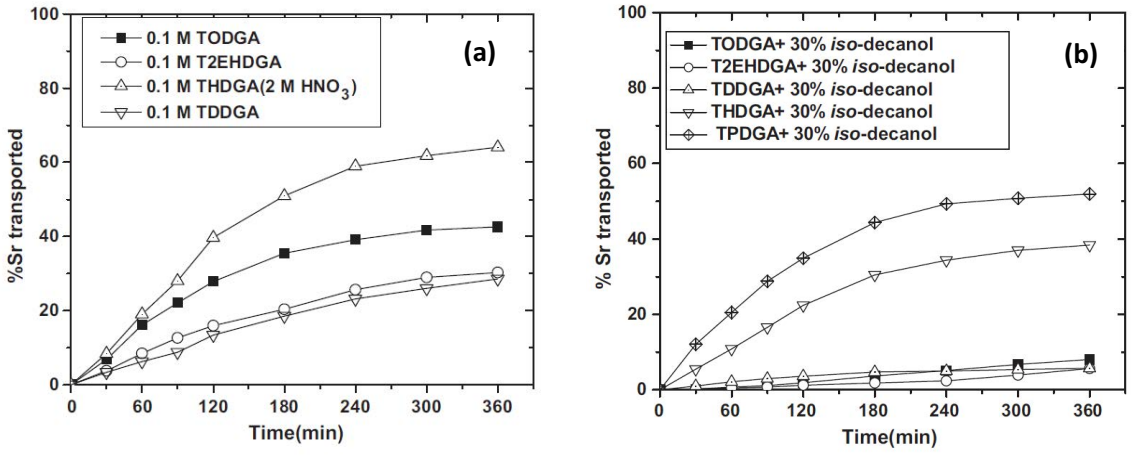

Fig. 11. Transport of Sr^{2+} by DGA-SLM in the absence (a), and in the presence (b) of phase modifier; feed phase: 3 M HNO_3; receiver phase: 0.1 M HNO_3. Reproduced with permission from the study of Panja et al. [40].

examples of multiple DGA ligands are shown in Fig. 2. One of the first studied multiple DGA ligands was synthesized by functionalizing 3 DGA units on a tripodal carbon platform (referred to as T-DGA) [65–68]. This ligand has shown significantly high extraction efficiency for trivalent actinides and lanthanides as compared to normal DGA ligands like TODGA. Due to the high extraction ability of this ligand, only 4 mM concentration of its solution was used for SLM studies [69] vis-a-vis 100 mM of TODGA. SLM studies with T-DGA yielded better results for the separation of Am^{3+} over UO_2^{2+} and Sr^{2+} as compared to TODGA [34–36]. The permeability coefficient of UO_2^{2+} with T-DGA was 6.09×10^{-5} cm/s, which is two orders of magnitude lower than the value with TODGA, giving better decontamination of the separated Am^{3+} over UO_2^{2+}. Good membrane stability was reported when the SLM was tested for over a week of continuous operation.

Contemporary to T-DGA, another tripodal DGA ligand was recently studied where 3 DGA units are functionalized on a *N*-pivot platform (referred to as DGA-TREN) with very interesting results [70–72]. Using 3 M HNO_3 as the feed and 4 mM ligand solution, the *D* values of metal ions followed the order: Pu^{4+} (18.5) > Am^{3+} (5.17) >> UO_2^{2+} (0.07), indicating that the selectivity of Am^{3+} and Pu^{4+} over UO_2^{2+} is better than T-DGA. Similar transport profiles were also observed with this ligand in SLM, where the transport followed the order: $Am^{3+} \sim Pu^{4+} >> UO_2^{2+}$ [73]. Utilizing the poor extraction properties of this ligand for hexavalent actinide ions, authors could effectively separate Am^{3+} from a mixture of Pu and U after oxidising Pu into Pu^{4+}. Later, Mahanty et al. [74] investigated the effect of alkyl substitution on N atom of DGA, and the effect of spacer between the *N*-pivot platform and the DGA moieties on the metal ion transport. Their SLM studies on the transport of Np^{4+} and Pu^{4+} suggested better transport rates with the *iso*-propyl substituted TREN-DGA as compared to the un-substituted ligand.

Subsequently, benzene-centered tripodal DGA (Bz-T-DGA) were evaluated for their metal ion extraction efficiency [75–77]. Mahanty et al. [78,79] studied a set of five Bz-T-DGA ligands as the carrier in SLM studies for the separation of Am^{3+}. Their work showed that the nature of alkyl substituents and the spacer length play a very important role in metal ion transport. The efficiency of the ligand decreased with increasing the alkyl spacer length between the benzene platform and the carbonyl groups of the DGA moieties. For example, the transport of Am^{3+} was 4.8 times slower in the ligand having ethylene ($-CH_2-CH_2-$) spacers than the ligand with methylene ($-CH_2-$) spacers [79].

There are also reports on metal ion transport studies using DGA functionalized calix[4]arene (C4DGA). Interesting results are reported with the C4DGA ligands having varying spacer lengths between the calix[4]arene platform and the DGA moieties, and having different substituents on the N atom of DGA [80–83]. Similarly, a large difference was seen in the efficiency of the ligands when DGA moieties were substituted on different sides of the calixarene scaffold (wide-rim, narrow-rim, and both side). One of the first reports on the flat sheet SLM studies with C4DGA ligands appeared almost a decade earlier where a wide-rim functionalized calix [4] arenes with 4 DGA units was used as the carrier extractant [84]. As shown in Fig. 12, with 1 mM of the C4DGA ligand solution, the transport of actinides followed the order: $Pu^{4+} > Am^{3+} > Pu^{3+} >> 9UO_2^{2+}$. The selectivity of Am^{3+} over UO_2^{2+} was about 10 times higher with the C4DGA ligands as compared to those seen with TODGA, and the tripodal DGA ligands such as T-DGA and DGA-TREN. Further investigations on the C4DGA ligands having upper-rim (narrow-rim), lower-rim (wide-rim), and both rim functionalized DGA units indicated that the narrow-rim functionalized C4DGA had a poor affinity for Am^{3+}, whereas the wide-rim and both side functionalized C4DGA showed similar affinities [85]. The binding affinity of these three ligands with lanthanide ions was also investigated in detail by spectroscopic methods [83]. In the case of the wide-rim functionalized C4DGA ligand, the four DGA moieties are attached to the calix [4] arene platform through the phenolic oxygens via a three-carbon atom spacer (Fig. 2). The overall four-atom space between the DGA sites and the rigid calix [4] arene platform provided better flexibility of the coordination sites, which eventually helped in better coordination with the metal ions. This argument was based on the results which revealed that the coordination ability of the C4DGA ligands decreased with a reducing number of spacer carbon atoms between the DGA moieties and the calix[4]arene platform [83]. In contrast, the DGA groups are directly attached to the calix [4] arene platform onto the narrow-rim of the scaffold, resulting in a poor flexibility of the pendant arms to induce a favourable orientation of their coordination sites. Accordingly, the binding ability of this ligand is several orders of magnitude lower than that of the C4DGA ligand with narrow-rim DGA functionalization. The results of the SLM studies [85] reported are in conformity of this explanation.

A systematic study was conducted to understand the effect of alkyl chain substitution in DGA moieties on the transport of metal ions [86]. To investigate this effect, only wide-rim functionalized C4DGA ligands were used. With the ligands having no substitution (L-I), *n*-propyl (L-II), *iso*-pentyl (L-III), and *n*-octyl (L-IV) substitutions, very interesting solvent extraction and SLM transport results of Am^{3+} were noted (Table 4). The D_{Am} values at 3 M HNO_3 followed

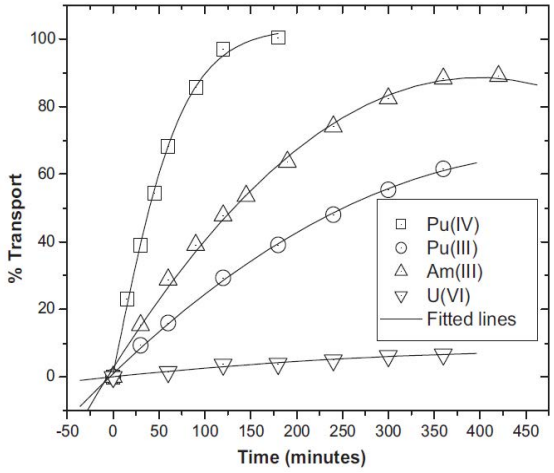

Fig. 12. Transport profiles of actinides with C4DGA-SLM. Feed: 3 M HNO_3; receiver: 0.01 M EDTA solution. Reproduced with permission from the study of Mohapatra et al. [84].

the order: 1.8 (L-I) < 80 (L-II) < 325 (L-III) ~ 402 (L-IV). The extraction efficiency of the ligands increased with the length of the alkyl chain tethered to the N atom up to *n*-pentyl, but became almost constant with the *n*-octyl group. The extraction efficiencies of these ligands were explained in the light of the orientation of the DGA pendant arm on the rigid calix [4] arene platform. It was assumed that in the absence of any substituent on the N atom of DGA, the pendant arm would not have any rotational restrictions and the coordinating sites of all the carbonyl 'O' atoms of the four DGA groups will not be pre-organized. This would eventually result in poor complexation ability of the ligand. On the other hand, after suitable alkyl substitution on the N-atom of the DGA moieties, as in L-II, L-III, and L-IV, the free rotation of the pendant arm would be restricted. This will eventually help in the pre-organization of the ligating sites in the ligand, and will result in better complexation. As shown in Fig. 13, these structural effects were also reflected in the SLM transport studies of Am^{3+}, where L-I yielded poor transport.

In continuation of the studies with the new multiple DGA ligands, a group of DGA-functionalized poly(propylene imine) diaminobutane dendrimers (Fig. 14) were also studied in flat sheet SLM [87]. These ligands were 0th, 1st, and 2nd generation dendrimers with 2, 4, and 8 DGA moieties appended onto the poly(propylene imine) diaminobutane scaffold. The SLM studies involved the transport of Am^{3+}, Pu^{4+}, Np^{4+}, UO_2^{2+}, and Sr^{2+} ions, which yielded poor results with the 0th generation ligand while the best results were obtained with the 2nd generation ligand. The performance of these ligands in the SLM was well explained in light of the extraction ability of these ligands which increased significantly with increasing the number of DGA functional groups.

Table 4
Distribution data of metal ions with 1 mmol/L C4DGA ligands [86]

Metal ions	Ionic size (Å)	Distribution ratio at 3 M HNO_3			
		L-I	L-II	L-III	L-IV
Am^{3+}	1.09	1.80	80.0	325	402
Eu^{3}	1.07	17.8	226	370	356
Pu^{4+}	0.96	9.67	53.6	68.4	47.0
Np^{4+}	0.98	2.72	35.2	–	41.2
UO_2^{2+}	1.4, 2.35	0.03	0.05	0.06	0.08

7.5. HFSLM studies with DGA

Authors have carried out a detailed study on 'actinide partitioning' using DGA ligands in the hollow fibre supported liquid membrane (HFSLM) configuration with encouraging results [20,88]. The studies included extensive investigation on the separation of Am^{3+} from feed solutions containing lanthanide surrogates and from tracer spiked simulated

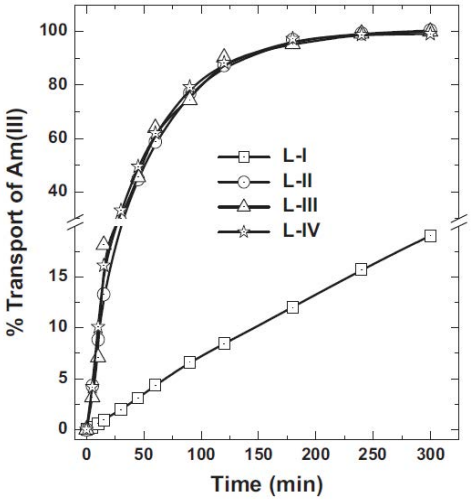

Fig. 13. Transport of Am^{3+} by C4DGA-SLM; carrier: 1 mmol/L; feed: 3 M HNO_3; strip: 0.01 M HNO_3. Reproduced with permission from the study of Ansari et al. [86].

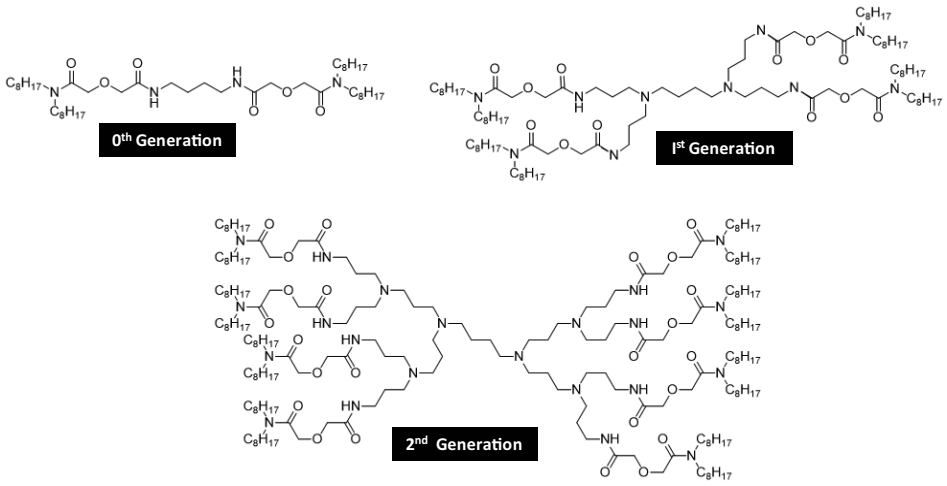

Fig. 14. Structures of 0th, 1st and 2nd generation DGA dendrimers.

HLW. An attempt was made to compare the performance of various extractants proposed for 'actinide partitioning' in HFSLM systems, where the transport of Am^{3+} was investigated in the presence of 0.6 g/L Nd (as surrogate for trivalent actinides and lanthanides) [89]. As shown in Fig. 15, quantitative transport of Am^{3+} was reported in 30 min with both TODGA and TEHDGA at 500 mL feed scale. Significantly fast transport of Am^{3+} with DGA extractants was correlated to the reasonably high D_{Am} values with these extractants (>100) at 3 M HNO_3 feed condition and very low D_{Am} values ((~10^{-3}) under receiver phase condition (0.01 M HNO_3). Under these conditions of feed and strip solutions, only ~65% Am^{3+} transport was observed for *N,N,N′,N′*-dimethyl dibutyl tetradecyl malonamide (DMDBTDMA, Fig. 16) due to relatively lower D_{Am} value (D_{Am} = 10 at 3 M HNO_3). Similarly, for the TRUEX solvent, which is a mixture of 0.2 M (phenyl))-*N,N*-diisobutyl carbamoyl methylene phosphine oxide (CMPO, Fig. 16) + 1.2 M TBP, only 50% transport of Am^{3+} was noticed in 20 min, beyond which a plateau was observed. It was observed that the strip phase acidity reached ~0.5 M HNO_3 in 60 min with TODGA, TEHDGA, and DMDBTDMA solvents, but it reached 0.7 M in just 20 min with the TRUEX solvent. Higher acid transport in this case was primarily due to the presence of relatively large concentrations of TBP (1.2 M). Apparently, the high D_{Am} value with CMPO at relatively lower acidities (0.2–0.5 M) hindered the stripping of metal ions in the receiver phase resulting in a plateau. The transport could not be improved even when a buffer mixture

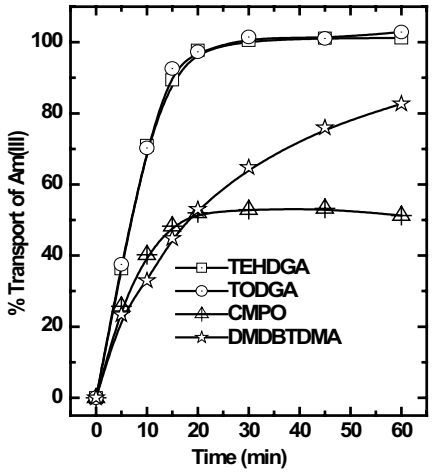

Fig. 15. Transport of Am^{3+} by HFSLM of different solvents; carriers: 0.1 M TODGA, 0.2 M TEHDGA, 1 M DMDBTDMA, and 0.2 M CMPO; feed: 0.6 g/L Nd at 3 M HNO_3 (500 mL); receiver: distilled water (500 mL); flow rate: 200 mL/min [89].

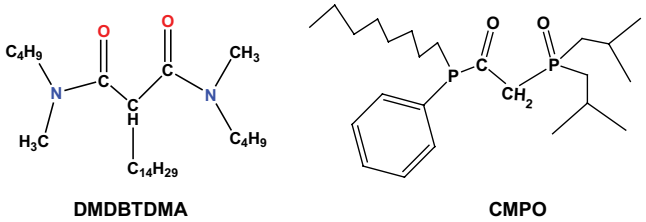

Fig. 16. Structure of DMDBTDMA and CMPO.

(0.4 M formic acid + 0.4 M hydrazine hydrate + 0.1 M citric acid [90]) was employed as the strip phase due to its limited buffer capacity. However, when the feed solution was 1 M or 3 M $NaNO_3$ (at pH 2), the transport was quantitative in just 20 min. These results confirmed that if CMPO has to be used for the transport of actinides from HLW, its acidity has to be controlled.

The performance of TODGA-HFSLM was investigated at a relatively higher scale (20 L) using Nd^{3+} in the feed solution [91]. It was observed that when the feed and the strip solutions were 0.5 L each, quantitative transfer of Nd was possible in just 30 min. However, about 18 h were necessary for the complete transport of Nd when the feed and the strip solutions were 20 L. When the volume of the strip solution was reduced to half (10 L), there was an acid build-up on the product side, which reduced the transport rate. The strip phase acidity was neutralized by the addition of alkali (NaOH) to get a cent percentage transport of the product.

In view of many folds higher extraction ability of the C4DGA ligands for Am^{3+} than those observed with TODGA, these ligands were studied in the HFSLM mode owing to the extremely low ligand inventory of this technique [88]. For a study employing radiotracer at 0.3 L scale with 0.18 m^2 surface area of hollow fibre contactor supported with 1 mmol/L C4DGA ligand, complete recovery of Am^{3+} was possible in 30 min [92]. The presence of Nd in the feed, however, suppressed the permeation rate, though it was not affected by changing the feed acidity (2–4 M HNO_3). The selectivity over other troublesome metal ions such as UO_2^{2+} and Sr^{2+} was found to be encouraging. Though the transport of the target Am^{3+} ion in the presence of the lanthanides was significantly affected, it was suggested to scale-up the process by using a larger size hollow fibre contactor with a higher surface area. The major hurdle envisaged at this point was the difficulty in applying the HFSLM technique to the actual radioactive actinide samples due to high radiation dose, but there should not be any issue for using HFSLM technique for the separation of lanthanides and transition elements.

8. Separation of Sr and Y with DGA-SLM

Yttrium-90 is one of the most widely studied radioisotopes in nuclear medicine research for the treatment of various cancers [93]. Due to its short half-life of 64.1 h, and its high energy of the emitted beta particle (E_{max} = 2.28 MeV), ^{90}Y is a widely accepted medical radio-isotope. Its beta particles can penetrate the soft tissues of cancer up to 1 cm. There are two ways ^{90}Y is obtained, either by neutron irradiation of natural yttrium or from the decay product of ^{90}Sr. Neutron irradiation of natural yttrium produces very low specific activity of ^{90}Y and is not suitable for radiopharmaceutical use. On the other hand, ^{90}Y being the daughter product of ^{90}Sr, it can be obtained in pure and carrier-free form from the decay product of ^{90}Sr ($T_{1/2}$~28.5 y). However, utmost care must be taken to get ^{90}Sr free ^{90}Y product as the former is a "bone-seeker", due to its chemical similarity with calcium.

It has been shown that DGA-based ligands show higher affinity for Y^{3+} over Sr^{2+} [15]. The extraction of Sr^{2+} basically increases with the feed acidity from 0.01 M HNO_3 to 3 M HNO_3 but decreases sharply from 3 M to 6 M HNO_3. On the other hand, the extraction of trivalent actinides, lanthanides,

and Y^{3+} continues to increase with increasing HNO_3 concentrations [94]. The best separation factor between Y^{3+} and Sr^{2+} is obtained at 6 M HNO_3, and therefore, a feed acidity of 6 M HNO_3 may be utilized for mutual separation of Sr^{2+} and Y^{3+} with DGA ligands. Looking at these features, TODGA and TEHDGA were explored for $^{90}Y/^{90}Sr$ separation in SLM. Dutta, et al. [95] evaluated different solvents for TODGA such as CCl_4, $CHCl_3$, hexone, 1-decanol, and xylene to get the best diluent for TODGA-SLM in terms of ^{90}Y product quality. Their studies yielded the best result with 0.1 M TODGA dissolved in $CHCl_3$ with a separation factor of 3.8×10^4 for Y^{3+} over Sr^{2+}. However, their SLM studies with TODGA/$CHCl_3$ system gave poor stability of the membrane due to the volatility issue of the solvent. Subsequent studies with TEHDGA-SLM in different diluents indicated the Y^{3+} transport trend: xylene > hexone > $CHCl_3$ > CCl_4 > 30% *iso*-decanol/*n*-dodecane [96]. The Sr^{2+} transport was also high in xylene, hexone, and CCl_4 media, resulting in poor product quality of ^{90}Y. Though the liquid–liquid extraction data gave better Sr/Y separation with TEHDGA vis-a-vis TODGA, the ligand gave poor results in SLM. In a recent study, an attempt was made to evaluate SLM for the separation of carrier-free ^{90}Y from ^{90}Sr using TODGA, and TEHDGA with lower concentration (10 moles/L) of the ligands [97]. At 6 M HNO_3, the separation factor (D_Y/D_{Sr}) of 11.7×10^4 and 4.0×10^3 was reported with TODGA and TEHDGA, respectively. At a feed acidity of 6 M HNO_3 and distilled water as the receiver phase, >95% ^{90}Y could be recovered selectively in 4 h with both ligands. The product, however, was contaminated with about 0.1% of Sr for both ligands. Nonetheless, medical grade ^{90}Y was obtained by passing the product through a Sr-selective commercial column. The authors emphasized that the separation of ^{90}Y from $^{90}Sr/^{90}Y$ mixture by DGA-SLM followed by column purification was a simple and good option to produce a medically pure ^{90}Y isotope on a larger scale.

Separation of carrier-free ^{90}Y from the mixture of $^{90}Y/^{90}Sr$ was also attempted with several calix[4]arene functionalized multiple DGA ligands (C4DGA) in flat sheet SLM [98]. The transports of both the elements, Sr and Y, were significantly lower at 6 M HNO_3 feed when compared with 3 M HNO_3. At 3 M HNO_3 as feed and 0.01 M EDTA or 0.01 M DOTA as the receiver, >97% Y^{3+} transport was noted in 6 h with negligible transport of Sr^{2+}. The purity of the ^{90}Y product was better with C4DGA-SLM vis-à-vis TODGA or TEHDGA-SLM. Additionally separated ^{90}Y products in the form of Y^{3+}–DOTA or Y^{3+}–EDTA may be directly used as radiopharmaceuticals.

9. Stability of SLMs

In SLMs, the ligand solutions are fixed inside the membrane support pores by weak capillary forces. Due to this, the stability and long-term use of SLMs are debatable. Due to the same reason, SLMs are not used at an industrial scale despite having several advantages. Instability of the SLMs may arise due to loss of the ligand from the support pores, which will eventually reduce the flux to an unacceptable level by the operator. The probable reasons for the loss of membrane phase from the pores of the support can be due to the (i) difference in the pressure on the two sides of the membrane, (ii) solubility of membrane phase in the feed or in the strip solutions, (iii) wetting of the membrane support by the aqueous phases, and creating water channels in the membrane, (iv) precipitation of the carrier or ML complex on the membrane surface thereby blocking the pores, (v) formation of emulsion due to mixing of membrane phase in water induced by lateral shear forces, and (vi) nature of the organic solvent used for dissolving the ligand. These listed reasons for SLM instability are intelligible. In many cases, any one of these reasons or a combination of a few may create SLM instability. One such example is dragging out the carrier from the pores of the membrane support when the pressure difference across the membrane exceeds a certain limit. Similarly, if the ligand dissolved in the membrane phase is water soluble, it will solubilize itself in the feed and strip solutions and will result in loss of membrane. Wett ability of the membrane support is also an important factor in deciding the SLM stability. If feed and strip solution can soak the support material, it will make water channels through the membrane. At the same time, the liquid membrane should be able to soak the hydrophobic ligand solution to make a stable SLM. The formation of coagulated species on the surface of the membrane will adversely affect the performance of the membrane due to pores blockage. This effect is more prominent with the ligand that forms the third phase. Sometimes if the stirring speeds in the feed or the strip compartments are very high, this will create a shear force at the membrane surface, and as a result, the ligand solution will come out of the pores by forming an emulsion. It is also proven that the SLM stability is significantly influenced by the volatility, viscosity, and miscibility of the solvent used for dissolving the ligand. Few solvents like chloroform are volatile and come out of the membrane support, thus giving poor stability to the SLM. Similarly, solvents like nitrobenzene may also react with feed or strip phase acid leading to its elimination from the membrane pores. Needless to mention that by analyzing the above discussions, one can easily deal with the stability of SLMs.

The effect of membrane support architecture also has a role in the overall transport in SLM. In general, the permeability coefficient (P) of a diffusing species in a porous polymeric matrix is correlated with the pore size, and tortuosity [99]:

$$P = \frac{\varepsilon R^2}{2\tau d_o} \tag{11}$$

where R = radius of the pore, τ = tortuosity, and d_o = membrane thickness. According to the above equation, the higher the pore size lower the resistance experienced by the complex species, and therefore, the permeation of the species should increase. However, this equation is true only when membranes of very small pore size are considered. Practically, it has been shown that with increasing the pore size of the membrane support, the transport rate decreases [52]. Since the liquid membrane component is simply held inside the pores of the membrane by capillary forces, increasing the pore size beyond a threshold would adversely affect the affinity of the ligand inside the membrane [100]. This phenomenon can be expressed by Laplace's equation, which correlates the minimum trans-membrane pressure (p) required to displace the extractant out of the membrane pore with the pore radius, R.

$$p = \left(\frac{2\gamma}{R}\right)\cos\theta \quad (12)$$

where γ is the interfacial tension between the solvent and water, and θ is the contact angle. With increasing pore size, the possibility of carrier molecules getting ejected out of the pores becomes more favourable. This effect indeed leads to a decrease in the carrier content in the pores and hence, is reflected in lowering the transport, and in several cases, this effect is prominent [101]. It was also demonstrated that the transport of actinides indeed decreased by increasing the membrane pore size as shown in Table 5.

10. Merits and demerits of SLM

Though the previous sections dealt with metal ion transport by SLMs and the results appeared quite promising, but the discussion on SLMs will be incomplete without knowing the merits and demerits of this technique. A few advantages of SLM technique are: (i) in SLM, the extraction and stripping take place simultaneously. This is in contrast to the conventional solvent extraction method, where extraction and stripping are done in two independent unit operation, (ii) SLM technique uses an extremely low amounts of organic solvents, and ligands that are impregnated in the pores of the membrane support. Therefore, the SLM technique will be a judicious choice for using very expensive and exotic ligands, (iii) since an extremely low amount of organic solvent is used in SLM, the generation of secondary organic waste is very low vis-à-vis conventional solvent extractionand (iv) SLM technique is relatively easy to scale-up and cost of operation is low. The efficiency of the SLM process, by and large, depends on the surface area, which can be easily tuned by using hollow fibre membrane modules of the desire size and having the desire number of fibres. Hollow fibre membrane modules are commercially available having a wide range of surface area from a few tenth of a square centimeter to a few square meters.

Despite several advantages listed above, the SLM technique has not been perceived its commercial application by the separation industry. The major reason for this is its limited long-term stability, and the issues related to the process scaling-up. From the SLM stability point of view, many volatile organic ligands or their solutions cannot be used. Similarly, ligands which have solubility in high polar solvents may not be useful for SLM application. One of the most important factors that limit the industrial application of the SLM technique is due to the lack of application-oriented research on the subject as industrial researchers mainly focus on the well-established hydrometallurgical processes such as solvent extraction and chromatography.

Table 5
Effect of pore size of membrane support on permeation of Am^{3+} by SLM

Pore size (mm)	Permeability coefficient (P), cm/s [84]	
	0.1 M TODGA	0.001 M C4DGA
0.20	20.4×10^{-4}	4.11×10^{-4}
0.45	13.7×10^{-4}	5.04×10^{-4}
1.2	12.3×10^{-4}	4.71×10^{-4}
5.0	9.17×10^{-4}	5.40×10^{-4}

11. Polymer inclusion membranes with DGA ligands

As discussed in the previous section, one of the main causes of liquid membrane instability in SLM is due to the loss of impregnated ligands from the membrane support. Such losses occur due to the solubility of the carrier and solvent in the surrounding solutions by forming emulsion droplets or due to differential pressure across the membrane. To overcome this problem, and to attain higher stability of the membrane, Sugiura et al. [102–108] prepared a series of plasticized cellulose triacetate (CTA) membranes containing carrier molecules for metal ion transport involving a mechanism similar to that operates in SLM. These membranes are referred to as polymer inclusion membranes (PIM) as the carrier ligands are immobilized inside the polymer matrix. Here, the plasticizer used in preparing the membrane acts as an organic solvent similar to those in SLM. Schow et al. [103] reported higher stability of PIMs than those of analogous SLMs. They observed no leaching of carrier solvent for a transport experiment continuously run for three months. Other workers have also confirmed the stability and durability of PIMs better than SLMs [104]. However, the permeability of metal ions is poor in the PIMs as compared to SLMs due to the more viscous polymeric membrane phase in the former.

Looking at the better stability of PIMs over SLMs, a few studies have also been performed in this area using various DGA ligands such as TODGA, TEHDGA, T-DGA, and C4DGA. It was found that the flux for the diffusion of Am^{3+} through TODGA-PIM containing CTA as a polymeric base and NPOE (2-nitrophenyl octyl ether) as plasticizer were poor when compared with those obtained in SLM experiments [120108]. Similar poor flux was also reported for TEHDGA-PIM [106]. Raut et al. [107] prepared TODGA-PVC-NPOE PIMs with varying compositions. As shown in Table 6, the best results were obtained with a composition of PIM containing 25% PVC. SThe sability of the membrane was good up to 14 d of continuous use. However, after 14 d, the performance of PIM started decreasing significantly, the reason for which was found to be swelling of the membrane when kept in contact with 3 M HNO_3. Mahanty et al. [108] carried out a series of studies for optimizing the TODGA-PIM composition with

Table 6
Optimization of PIM composition for Am^{3+} transport. Feed: 3 M HNO_3 (20 mL); receiver: 0.1 M 2-hydroxy isobutyramide (20 mL) [107]

Membrane composition	% Am^{3+} transport in 4 h
15.5% TODGA + 37.5% PVC + 47% NPOE	67.6
27% TODGA + 32.5% PVC + 40.5% NPOE	91.0
8% TODGA + 26% PVC + 66% NPOE	84.5
16.5% TODGA + 33.5% PVC + 50% NPOE	98.0
12.5% TODGA + 25% PVC + 62.5% NPOE	99.7

CTA base material and NPOE plasticizer. It was found that a composition of 58% TODGA + 30% NPOE + 12% CTA was the best composition. They prepared a series of PIMs containing three different DGA ligands, viz. *N,N,N′,N′*-tetra-*n*-pentyl DGA (TPDGA), *N,N,N′,N′*-tetra-*n*-hexyl DGA (THDGA) and *N,N,N′,N′*-tetra-*n*-decyl DGA (TDDGA), and evaluated them for the separation of actinide ions such as Am^{3+}, Pu^{4+}, Th^{4+} and UO_2^{2+} [109]. The best membrane composition was 68.4% DGA + 17.9% NPOE + 13.7% CTA for all three ligands. It was noted that TPDGA and THDGA gave uniform and homogeneous membrane, as ascertained by Transmission Infrared Mapping Microscopy (TIMM), but TDDGA gave a non-homogeneous membrane (Fig. 17). Even the ligand leached out of the membrane for TDDGA-PIM during the transport experiment. A reason for this could not be confirmed.

A CTA-based PIM containing the T-DGA ligand was also prepared and studied for the uptake of actinides from acidic feed solutions [110]. This study was performed as a part of sensor development for actinides. The PIM containing 25.6% T-DGA, 53.9% NPOE, and 20.5% CTA yielded the actinide uptake in the order: $Pu^{4+} > Am^{3+} > Th^{4+} > UO_2^{2+}$, which was identical with the results observed with TODGA and TEHDGA-PIMs. Similarly, CTA-based PIMs containing C4DGA ligands were evaluated for the separation of actinides (Am^{3+}, Pu^{4+}, Th^{4+}, and UO_2^{2+}) from dilute nitric acid feed solutions [111]. The optimized PIM composition was 6.5% C4DGA, 67.7% NPOE, and 25.8% CTA. At 1 M HNO_3 feed and 0.1 M a-HIBA receiver, the transport efficiency followed the order: $Pu^{4+} > Am^{3+} > Th^{4+}$ with no detectable transport of UO_2^{2+} ion. The diffusion coefficient and permeability coefficient of Am^{3+} were several times lower than those observed in SLM, obviously due to the higher viscosity of the diffusion medium in PIM.

12. Conclusions and perspectives

The supported liquid membrane (SLM) technique is an emerging separation technique that appears promising and attractive for hydrometallurgical separation processes. Looking at the numerous advantages of the SLM technique, for example, low cost and ease of operation with extremely low ligand inventory and low energy consumption, the technique may be attractive for operation with exotic ligands. Despite the advantages, the major challenge has been the SLM stability which has not been so critical in SLMs containing DGA ligands. This could be due to the type of diluents (*n*-dodecane) used for DGA ligands which have no wettability issues and also are not usually leached out of the membrane pores. Though the studies with DGA-based SLMs have been quite satisfactory for actinides and lanthanides, extensive and dedicated research is the need of the hour to look at several important parameters for their actual applications. One advantage of the DGAs is their exceptionally high extraction efficiency which gives very high mass transfer rates under normal operating conditions.

One of the important areas that need through investigations is the development of hydrophobic membranes, both flat sheet and hollow fibres that must show reasonably good

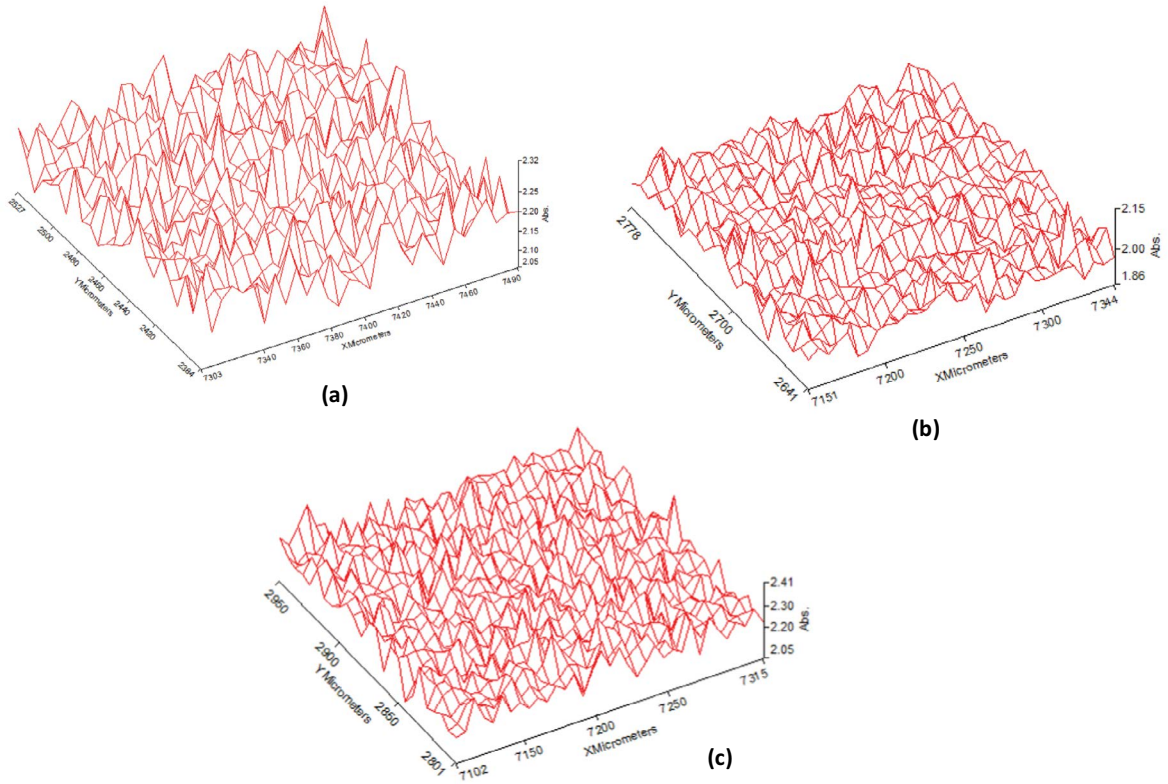

Fig. 17. TIMM distribution profile of CTA based PIMs: (a) blank membrane recorded at 1,529 cm^{-1}, (b) TPDGA, and (c) THDGA membrane recorded at 1,645 cm^{-1}. Reproduced with permission from the study of Mahanty et al. [109].

radiation stability. At present, the commercial hollow fibre membrane modules are made up of polypropylene that has limited radiation stability of about 500 KGy. One may look into the possibility of exploring membranes made up of the materials like polysulfone and polyethersulfone which have better radiation stability. One may also explore the ceramic membranes having hydrophobic pores for holding the liquid membrane (carrier solution). Alternatively, the carrier ligands may be fixed inside the pores of ceramic membranes, either by functionalizing the ligands chemically or by the polymer inclusion technique. Needless to mention that the ceramic membranes will be the most sought for applications in the nuclear industry due to the radiation issues encountered in those industries.

The application of SLM-based methods is completely dependent on the use of selective ligands. There is a scope for organic synthesis researchers who are designing and synthesizing new ligands for the selective separation of target elements. The use of the SLM technique for their metal ion separation studies will be an advantage as the experiment can be performed with extremely low ligand inventory and with a simple transport cell. The results of flat sheet SLM studies may be scaled-up for real application in the HFSLM technique. Another interesting prospect of the SLM method is the preparation of analytical samples. Here, the analytes from a large volume of the sample can be concentrated in very small volumes either by flat sheet SLM or by liquid phase micro-extraction using hollow fibres. The other important issue that needs to address is the automation of the SLM technique for high throughput in real applications or in analytical applications.

References

[1] S.A. Ansari, P.K. Mohapatra, A review on solid phase extraction of actinides and lanthanides with amide based extractants, J. Chromatogr. A, 1499 (2017) 1–20.

[2] M. Sethurajan, E.D. Van Hullebusch, D. Fontana, A. Akcil, H. Deveci, B. Batinic, J.P. Leal, T.A. Gasche, M.A. Kucuker, K. Kuchta, I.F.F. Neto, H.M. Soares, A. Chmielarz, Recent advances on hydrometallurgical recovery of critical and precious elements from end of life electronic wastes – a review, Critical Rev. Environ. Sci. Technol., 49 (2019) 212–275.

[3] M. Amini, A. Rahbar-Kelishami, M. Alipour, O. Vahidi, Supported liquid membrane in metal ion separation: an overview, J. Membr. Sci. Res., 4 (2018) 121–135.

[4] G.S. Su, N. Morad, N. Ismail, M. Rafatullah, Developments in supported liquid membranes for treatment of metal-bearing wastewater, Sep. Purif. Rev., 51 (2022) 38–56.

[5] T.A. Kurniawan, M.H.D. Othman, D. Singh, R. Avtar, G.H. Hwang, T. Setiadi, W. Lo, Technological solutions for long-term storage of partially used nuclear waste: a critical review, Ann. Nucl. Energy, 166 (2022) 108736, doi: 10.1016/j.anucene.2021.108736.

[6] International Approaches for Nuclear Waste Disposal in Geological Formations: Geological Challenges in Radioactive Waste Isolation—Fifth Worldwide Review, US-DOE Report 2017. Available at: https://doi.org/10.2172/1353043

[7] R. Taylor, Reprocessing Recycling of Spent Nuclear Fuel, Woodhead Publishing, Cambridge, UK, 2015, ISBN 978-1-78242-212-9.

[8] P. Baron, S.M. Cornet, E.D. Collins, G. DeAngelis, J.P. Glatz, V. Ignatiev, T. Inoue, A. Khaperskaya, I.T. Kim, M. Kormilitsyn, T. Koyama, J.D. Law, H.S. Lee, K. Minato, Y. Morita, J. Uhlir, D. Warin, R. Taylor, A review of separation processes proposed for advanced fuel cycles based on technology readiness level assessments, Prog. Nucl. Energy, 117 (2019) 103091, doi: 10.1016/j.pnucene.2019.103091.

[9] C.C. Pascal, M. Tiphine, G. Krivtchik, D. Freynet, C. Cany, R. Eschbach, C. Chabert, COSI6: a tool for nuclear transition scenario studies and application to SFR deployment scenarios with minor actinide transmutation, Nucl. Technol., 192 (2015) 91–110.

[10] A. Salvatores, Nuclear fuel cycle strategies including partitioning and transmutation, Nucl. Eng. Des., 235 (2005) 805–816.

[11] Y. Gohar, Y. Cao, A.R. Kraus, ADS design concept for disposing of the U.S. spent nuclear fuel inventory, Ann. Nucl. Energy, 160 (2021) 108385, doi: 10.1016/j.anucene.2021.108385.

[12] S.A. Ansari, P.N. Pathak, P.K. Mohapatra, V.K. Manchanda, Chemistry of diglycolamides: Promising extractants for actinide partitioning, Chem. Rev., 112 (2012) 1751–1772.

[13] D. Whittaker, A. Geist, G. Modolo, R. Taylor, M. Sarsfield, A. Wilden, Applications of diglycolamide based solvent extraction processes in spent nuclear fuel reprocessing, Part 1: TODGA, Solvent Extr. Ion Exch., 36 (2018) 223–256.

[14] D. Magnusson, B. Christiansen, J.P. Glatz, R. Malmbeck, G. Modolo, D. Purroy, C. Sorel, Demonstration of a TODGA based extraction process for the partitioning of minor actinides from a PUREX raffinate. Part III: centrifugal contactor run using genuine fuel solution, Solvent Extr. Ion Exch., 27 (2009) 26–35.

[15] Z. Zhu, Y. Sasaki, H. Suzuki, S. Suzuki, T. Kimura, Cumulative study on solvent extraction of elements by *N,N,N′,N′*-tetraoctyl-3-oxapentanediamide (TODGA) from nitric acid into *n*-dodecane, Anal. Chim. Acta, 527 (2004) 163–168.

[16] M.P. Jensen, T. Yaita, R. Chiarizia, Reverse-micelle formation in the partitioning of trivalent *f*-element cations by biphasic systems containing a tetraalkyl diglycolamide, Langmuir, 23 (2007) 4765−4774.

[17] T. Yaita, A.W. Herlinger, P. Thiyagarajan, M.P. Jensen, Influence of extractant aggregation on the extraction of trivalent *f*-element cations by a tetraalkyl diglycolamide, Solvent Extr. Ion Exch., 22 (2004) 533–571.

[18] A. Leoncini, S.A. Ansari, P.K. Mohapatra, J. Huskens, W. Verboom, Diglycolamide-functionalized poly(propylene imine) diaminobutane dendrimers for sequestration of trivalent f-elements: synthesis, extraction and complexation, Dalton Trans., 46 (2017) 501–508.

[19] S.A. Ansari, P.K. Mohapatra, A. Leoncini, S.M. Ali, A. Singhadeb, J. Huskens, W. Verboom, Unusual extraction of trivalent f-cations using diglycolamide dendrimers in a room temperature ionic liquid: extraction, spectroscopic and DFT studies, Dalton Trans., 46 (2017) 16541–16550.

[20] S.A. Ansari, P.K. Mohapatra, Hollow fibre supported liquid membranes for nuclear fuel cycle applications: a review, Cleaner Eng. Technol., 4 (2021) 100138.

[21] A.K. Pabby, B. Swain, N.L. Sonar, V.K. Mittal, T.P. Valsala, S. Ramsubramanian, D.B. Sathe, R.B. Bhatt, S. Pradhan, Radioactive waste processing using membranes: state of the art technology, challenges and perspectives, Sep. Purif. Rev., 51 (2022) 143–173.

[22] J.V. Carolan, Separation of actinides from spent nuclear fuel: a review, J. Hazard. Mater., 318 (2016) 266–281.

[23] S.A. Ansari, P.N. Pathak, P.K. Mohapatra, V.K. Manchanda, Aqueous partitioning of minor actinides by different processes, Sep. Purif. Rev., 40 (2011) 43–76.

[24] K.L. Nash, C. Madic, J.N. Mathur, J. Lacquement, In: L.R. Morss, N.M. Edelstein, J. Fuger J.J. Katz, Eds., The Chemistry of the Actinide and Transactinide Elements, Vol. 4, 3rd ed., Springer, The Netherlands, 2006, pp. 2622–2798.

[25] A.K. Pabby, S. Rizvi, A.M. Sastre, Handbook of Membrane Separations, Chemical, Pharmaceutical, Food and Biotechnological Applications, 2nd ed., CRC Press, Boca Raton, Florida, USA, 2015, ISBN: 978-1-4665-5556-3.

[26] G.R. Bolton, A.W. Boesch, J. Basha, D.P. LaCasse, B.D. Kelley, H. Acharya, Effect of protein and solution properties on the Donnan effect during the ultrafiltration of proteins, Biotechnol. Prog., 27 (2011) 140–152.

[27] G.B. Diller, In: Recycling in Textiles, Woodhead Publishing Series in Textiles, 2006, pp. 95–113.
[28] K. Baek, B.K. Kim, H.J. Cho, J.W. Yang, Removal characteristics of anionic metals by micellar-enhanced ultrafiltration, J. Hazard. Mater., 99 (2003) 303–311.
[29] R.S. Juang, Y.Y. Xu, C.L. Chen, Separation and removal of metal ions from dilute solutions using micellar-enhanced ultrafiltration, J. Membr. Sci., 218 (2003) 257–267.
[30] K. Trivunac, S. Stevanovic, Removal of heavy metal ions from water by complexation-assisted ultrafiltration, Chemosphere, 64 (2006) 486–491.
[31] R.S. Juang, R.C. Shiau, Metal removal from aqueous solutions using chitosan-enhanced membrane filtration, J. Membr. Sci., 165 (2000) 159–167.
[32] P.R. Danesi, E.P. Horwitz, P.G. Rickert, Rate and mechanism of facilitated americium(III) transport through a supported liquid membrane containing a bifunctional organophosphorus mobile carrier, J. Phys. Chem., 87 (1983) 4708–4715.
[33] C.R. Wilke P. Chang, Correlation of diffusion coefficients in dilute solutions, AlChE J., 1 (1955) 264–270.
[34] S.A. Ansari, P.K. Mohapatra, D.R. Prabhu, V.K. Manchanda, Transport of Americium(III) through a supported liquid membrane containing *N,N,N′,N′*-tetraoctyl-3-oxapentane diamide (TODGA) in *n*-dodecane as the carrier, J. Membr. Sci., 282 (2006) 133–141.
[35] S.A. Ansari, P.K. Mohapatra, D.R. Prabhu, V.K. Manchanda, Evaluation of *N,N,N′,N′*-tetraoctyl-3-oxapentane-diamide (TODGA) as a mobile carrier in remediation of nuclear waste using supported liquid membrane, J. Membr. Sci., 298 (2007) 169–174.
[36] S.A. Ansari, P.K. Mohapatra, D.R. Prabhu, V.K. Manchanda, Transport of lanthanides and fission products through supported liquid membranes containing *N,N,N′,N′*-tetraoctyl diglycolamide (TODGA) as the carrier, Desalination, 232 (2008) 254–261.
[37] S. Panja, P.K. Mohapatra, P. Kandwal, S.C. Tripathi, V.K. Manchanda, Pertraction of plutonium in the +4 oxidation state through a supported liquid membrane containing TODGA as the carrier, Desalination, 262 (2010) 57–63.
[38] S. Panja, P.K. Mohapatra, S.C. Tripathi, V.K. Manchanda, Controlled pertraction of Pu(III) under reducing conditions from acidic feeds using TODGA as the carrier extractant, Sep. Sci. Technol., 46 (2011) 94–104.
[39] S. Panja, P.K. Mohapatra, S.C. Tripathi, G.D. Dhekane, P.M. Gandhi, P. Janardan, Liquid–liquid extraction and pertraction of Eu(III) from nitric acid medium using several substituted diglycolamide extractants, Sep. Sci. Technol., 48 (2013) 2179–2187.
[40] S. Panja, P.K. Mohapatra, S.C. Tripathi, G.D. Dhekane, P.M. Gandhi, P. Janardan, Liquid–liquid extraction and pertraction behavior of Am(III) and Sr(II) with diglycolamide carrier extractants, J. Membr. Sci., 399–400 (2012) 28–36.
[41] S. Panja, R. Ruhela, S.K. Misra, J.N. Sharma, S.C. Tripathi, A. Dakshinamoorthy, Facilitated transport of Am(III) through a flat-sheet supported liquid membrane (FSSLM) containing tetra(2-ethyl hexyl) diglycolamide (T2EHDGA) as carrier, J. Membr. Sci., 325 (2008) 158–165.
[42] S. Panja, P.K. Mohapatra, S.C. Tripathi, V.K. Manchanda, Facilitated transport of uranium(VI) across supported liquid membranes containing T2EHDGA as the carrier extractant, J. Hazard. Mater., 188 (2011) 281–287.
[43] S. Panja, P.K. Mohapatra, S.K. Misra, S.C. Tripathi, Carrier facilitated transport of europium(III) across supported liquid membranes containing *N,N,N′,N′*-tetra-2-ethylhexyl-3-oxapentane-diamide (T2EHDGA) as the extractant, Sep. Sci. Technol., 46 (2011) 1941–1949.
[44] S. Panja, P.K. Mohapatra, P. Kandwal, S.C. Tripathi, Uranium(VI) pertraction across a supported liquid membrane containing a branched diglycolamide carrier extractant: Part III. Mass transfer modelling, Desalination, 285 (2012) 213–218.
[45] S. Panja, P.K. Mohapatra, S.C. Tripathi, Facilitated transport of U(VI) across supported liquid membranes (SLM) containing T2EHDGA: Part II. Nature of feed, pore size and temperature on pertraction rates, Desal. Water Treat., 38 (2012) 207–214.
[46] Y. Sasaki, Y. Sugo, S. Suzuki, S. Tachimori, The novel extractants diglycolamides for the extraction of lanthanides and actinides in HNO3-n-dodecane system, Solvent Extr. Ion Exch., 19 (2001) 91–103.
[47] S. Tachimori, Y. Sasaki, S. Suzuki, Modification of TODGA-*n*-dodecane solvent with a monoamide for high loading of lanthanides(III) and actinides(III), Solvent Extr. Ion Exch., 20 (2002) 687–699.
[48] Y. Sugo, Y. Sasaki, S. Tachimori, Studies on hydrolysis and radiolysis of *N,N,N′,N′*-tetraoctyl-3-oxapentane-1,5-diamide, Radiochim. Acta, 90 (2002) 161–165.
[49] E.A. Mowafy, H.F. Aly, Synthesis of some *N,N,N′,N′*-tetraalkyl-3-oxa-pentane-1,5-diamide and their applications in solvent extraction, Solvent Extr. Ion Exch., 25 (2007) 205–224.
[50] K. Bell, A. Geist, F. McLachlan, G. Modolo, R. Taylor, A. Wilden, Nitric acid extraction into TODGA, Procedia Chem., 7 (2012) 152–59.
[51] S. Panja, P.K. Mohapatra, S.C. Tripathi, V.K. Manchanda, Transport of Th(IV) across a supported liquid membrane containing *N,N,N,N*-tetraoctyl-3-oxapentane-diamide (TODGA) as the extractant, Sep. Sci. Technol., 45 (2010) 1112–1120.
[52] S. Panja, P.K. Mohapatra, S.C. Tripathi, V.K. Manchanda, Studies on U(VI) pertraction across a *N,N,N′,N′*-tetraoctyl diglycolamide (TODGA) supported liquid membrane, J. Membr. Sci., 337 (2009) 274–281.
[53] R.B. Gujar, S.A. Ansari, M.S. Murali, P.K. Mohapatra, V.K. Manchanda, Comparative evaluation of two substituted diglycolamide extractants for actinide partitioning, J. Radioanal. Nucl. Chem., 284 (2010) 377–385.
[54] S.A. Ansari, P.N. Pathak, M. Hussain, A.K. Prasad, V.S. Parmar, V.K. Manchanda, *N,N,N′,N′*-tetraoctyl diglycolamide (TODGA): a promising extractant for actinide-partitioning from high-level waste (HLW), Solvent Extr. Ion Exch., 23 (2005) 463–479.
[55] R.B. Gujar, S.A. Ansari, P.K. Mohapatra, V.K. Manchanda, Development of T2EHDGA based process for actinide partitioning. Part-I: Batch studies for process optimization, Solvent Extr. Ion Exch., 28 (2010) 350–366.
[56] Y. Sasaki, Y. Sugo, S. Suzuki, T. Kimura, A method for the determination of extraction capacity and its application to *N,N,N′,N′*-tetraalkylderivatives of diglycolamide-monoamide/*n*-dodecane media, Anal. Chim. Acta, 543 (2005) 31–37.
[57] P.R.V. Rao, Z. Kolarik, A review of third phase formation in extraction of actinides by neutral organophosphorus extractants, Solvent Extr. Ion Exch., 14 (1996) 955–993.
[58] K. Rama Swami, K.A. Venkatesan, M.P. Antony, Role of phase modifiers in controlling the third-phase formation during the solvent extraction of trivalent actinides, Solvent Extr. Ion Exch., 37 (2019) 500–517.
[59] R.B. Gujar, S.A. Ansari, D.R. Prabhu, P.N. Pathak, S.K. Thulasidas, P.K. Mohapatra, V.K. Manchanda, Actinide partitioning with a modified TODGA solvent: counter-current extraction studies with simulated high level waste, Solvent Extr. Ion Exch., 30 (2012) 156–170.
[60] R.B. Gujar, S.A. Ansari, D.R. Prabhu, D.R. Raut, P.N. Pathak, S.K. Thulasidas, P.K. Mohapatra, V.K. Manchanda, Demonstration of T2EHDGA based process for actinide partitioning. Part-II: counter-current extraction studies, Solvent Extr. Ion Exch., 28 (2010) 764–777.
[61] S.A. Ansari, P.K. Mohapatra, S.M. Ali, N. Rawat, B.S. Tomar, A. Leoncini, J. Huskens, W. Verboom, Complexation thermodynamics of tetraalkyl diglycolamides with trivalent f-elements in ionic liquid: spectroscopic, microcalorimetric and computational studies, New J. Chem., 42 (2018) 708–716.
[62] S.A. Ansari, R.B. Gujar, P.K. Mohapatra, Complexation of tetraalkyl diglycolamides with trivalent *f*-cations in a room temperature ionic liquid: extraction and spectroscopic investigations, Dalton Trans., 146 (2017) 7584–7593.
[63] S.A. Ansari, D. Rama Mohana Rao, P.K. Mohapatra, First report on the complexation of uranyl ion with two diglycolamide ligands in a room temperature ionic liquid: optical spectroscopy and calorimetric studies, Chem. Select., 6 (2021) 6037–6042.
[64] S.A. Ansari, A.P. Wadawale, W. Verboom, P.K. Mohapatra, Isolation of single crystals of homoleptic UO_2^{2+}-diglycolamide

complex from a room temperature ionic liquid: X-ray crystallography and complexation studies, New J. Chem., 46 (2022) 950–954.
[65] K. Matloka, A. Gelis, M. Regalbuto, G. Vandegrift, M.J. Scott, C3-symmetric tripodal thio/diglycolamide-based ligands for trivalent *f*-element separations, Sep. Sci. Technol., 41 (2006) 2129–2146.
[66] K. Matloka, A. Gelis, M. Regalbuto, G. Vandegrift, M.J. Scott, Highly efficient binding of trivalent *f*-elements from acidic media with a C3-symmetric tripodal ligand containing diglycolamide arms, Dalton Trans., 2005, 3719–3721.
[67] D. Janczewski, D.N. Reinhoudt, W. Verboom, C. Hill, C. Allignol, M.T. Duchesne, Tripodal diglycolamides as highly efficient extractants for *f*-elements, New J. Chem., 32 (2008) 490–495.
[68] S.A. Ansari, P.K. Mohapatra, W. Verboom, L. Rao, Thermodynamics of biphasic lanthanide extraction by tripodal diglycolamide: a solution calorimetry study, Dalton Trans., 45 (2016) 17216–17222.
[69] P.K. Mohapatra, I. Iqbal, D.R. Raut, W. Verboom, J. Huskens, V.K. Manchanda, Evaluation of a novel tripodal diglycolamide for actinide extraction: solvent extraction and SLM transport studies, J. Membr. Sci., 375 (2011) 141–149.
[70] A. Leoncini, P.K. Mohapatra, A. Bhattacharyya, D.R. Raut, P.K. Verma, N. Tiwari, D. Bhattacharyya, S.N. Jha, A.M. Wouda, J. Huskens, W. Verboom, Unique selectivity reversal in Am^{3+}-Eu^{3+} extraction in a tripodal TREN-based diglycolamide in ionic liquid: extraction, luminescence, complexation and structural studies, Dalton Trans., 45 (2016) 2476–2484.
[71] S.A. Ansari, P.K. Mohapatra, A. Leoncini, S.M. Ali, J. Huskens, W. Verboom, Highly efficient N-pivot tripodal diglycolamide ligands for trivalent *f*-cations: synthesis, extraction, spectroscopy and density functional theory studies, Inorg. Chem., 58 (2019) 8633–8644.
[72] S.A. Ansari, P.K. Mohapatra, P.K. Verma, A. Leoncini, A.K. Yadav, S.N. Jha, D. Bhattacharyya, J. Huskens, W. Verboom, Highly efficient extraction of trivalent *f*-cations using several N-pivot tripodal diglycolamide ligands in an ionic liquid: the role of ligand structure on metal ion complexation, Eur. J. Inorg. Chem., 2020 (2020) 191–199.
[73] B. Mahanty, S.A. Ansari, P.K. Mohapatra, A. Leoncini, J. Huskens, W. Verboom, Liquid–liquid extraction and facilitated transport of *f*-elements using an N-pivot tripodal ligand, J. Hazard. Mater., 347 (2018) 478–485.
[74] B. Mahanty, P.K. Verma, P.K. Mohapatra, A. Leoncini, J. Huskens, W. Verboom, Pertraction of Np(IV) and Pu(IV) across a flat sheet supported liquid membrane containing two N-pivoted tripodal diglycolamides, Sep. Purif. Technol., 238 (2020) 116418, doi: 10.1016/j.seppur.2019.116418.
[75] S.A. Ansari, A. Leoncini, P.K. Mohapatra, J. Huskens, W. Verboom, Effect of alkyl substituent and spacer length in benzene-centred tripodal diglycolamides on the sequestration of minor actinides, Dalton Trans., 47 (2018) 13631–13640.
[76] A. Leoncini, S.A. Ansari, P.K. Mohapatra, A. Boda, S.M. Ali, J. Huskens, W. Verboom, Benzene-centered tripodal diglycolamides: Synthesis, metal ion extraction, luminescence spectroscopy and DFT studies, Dalton Trans., 46 (2017) 1431–1438.
[77] S.A. Ansari, P.K. Mohapatra, A. Leoncini, J. Huskens, W. Verboom, Benzene-centred tripodal diglycolamides for sequestration of trivalent actinides: metal ion extraction and luminescence spectroscopic investigations in room temperature ionic liquid, Dalton Trans., 46 (2017) 11355–11362.
[78] B. Mahanty, P.K. Mohapatra, A. Leoncini, J. Huskens, W. Verboom, Evaluation of three novel benzene-centered tripodal diglycolamide ligands for the pertraction of americium(III) through flat sheet membranes for nuclear waste remediation applications, Sep. Purif. Technol., 229 (2019) 115846, doi: 10.1016/j.seppur.2019.115846.
[79] B. Mahanty, P.K. Verma, P.K. Mohapatra, A. Leoncini, J. Huskens, W. Verboom, Pertraction of americium(III) through supported liquid membranes containing benzene-centered tripodal diglycolamides (Bz-T-DGA) as an extractant, Chem. Eng. Res. Des., 141 (2019) 84–92.
[80] P.K. Mohapatra, M. Iqbal, D.R. Raut, W. Verboom, J. Huskens, S.V. Godbole, Complexation of novel diglycolamide functionalized calix[4]arenes: unusual extraction behaviour, transport, and fluorescence studies, Dalton Trans., 41 (2012) 360–363.
[81] M. Iqbal, P.K. Mohapatra, S.A. Ansari, J. Huskens, W. Verboom, Preorganization of diglycolamides on the calix[4]arene platform and its effect on the extraction of Am(III)/Eu(III), Tetrahedron, 68 (2012) 7840–7847.
[82] S.A. Ansari, S.M. Ali, A. Sengupta, A. Bhattacharyya, P.K. Mohapatra, W. Verboom, Understanding the complexation of Eu^{3+} with three diglycolamide-functionalized calix[4]arenes: spectroscopic and DFT studies, Dalton Trans., 45 (2016) 5425–5429.
[83] H. Huang, S. Ding, N. Liu, Y. Wu, D. Su, S. Huang, Extraction of trivalent americium and europium from nitric acid solution with a calixarene-based diglycolamide, Sep. Purif. Technol., 123 (2014) 235–240.
[84] P.K. Mohapatra, M. Iqbal, D.R. Raut, J. Huskens, W. Verboom, Unusual transport behaviour of actinide ions with a novel calix[4]arene-tetra-diglycolamide (C4DGA) extractant as the carrier, J. Membr. Sci., 411–412 (2012) 64–72.
[85] P.K. Mohapatra, D.R. Raut, M. Iqbal, J. Huskens, W. Verboom, A comparative evaluation of the liquid–liquid extraction and pertraction efficiency of a both-side diglycolamide-functionalized calix[4]arene with analogous upper and lower-rim calixarene for actinide separations, J. Membr. Sci., 444 (2013) 268–275.
[86] S.A. Ansari, P.K. Mohapatra, M. Iqbal, P. Kandwal, J. Huskens, W. Verboom, Novel diglycolamide functionalized calix[4] arenes for actinide extraction and supported liquid membrane studies: role of substituents in the pendant arms and mass transfer modeling, J. Membr. Sci., 430 (2013) 304–311.
[87] S.A. Ansari, P.K. Mohapatra, A. Leoncini, J. Huskens, W. Verboom, Diglycolamide-functionalized dendrimers: studies on Am(III) pertraction from radioactive waste, Sep. Purif. Technol., 187 (2017) 110–117.
[88] S.A. Ansari, P. Kandwal, P.K. Mohapatra, In: Handbook of Membrane Separations, Chemical, Pharmaceutical, Food and Biotechnological Applications, 2nd ed., CRC Press, Boca Raton, Florida, USA, 2015, pp. 787–812.
[89] S.A. Ansari, P.K. Mohapatra, D.R. Raut, T.K. Seshagiri, B. Rajeswari, V.K. Manchanda, Performance of actinide partitioning extractants in hollow fibre supported liquid membrane for the transport of actinides and lanthanides from high level nuclear waste, J. Membr. Sci., 337 (2009) 304–309.
[90] R.R. Chitnis, P.K. Wattal, A. Ramanujam, P.S. Dhami, V. Gopalakrishnan, A.K. Bauri, A. Banerji, Recovery of actinides extracted by TRUEX solvent from high level waste using complexing agents, J. Radioanal. Nucl. Chem., 240 (1999) 721–726.
[91] S.A. Ansari, R.B. Gujar, P.K. Mohapatra, P. Kandwal, S.K. Thulasidas, V.K. Manchanda, A 'cold' actinide partitioning run at 20 L scale with hollow fibre supported liquid membrane using diglycolamide extractants, Radiochim. Acta, 99 (2011) 815–821.
[92] S.A. Ansari, P.K. Mohapatra, P. Kandwal, W. Verboom, Diglycolamide-functionalized calix[4]arene for Am(III) recovery from radioactive wastes: liquid membrane studies using a hollow fibre contactor, Ind. Eng. Chem. Res., 55 (2016) 1740–1747.
[93] N. Khajornjiraphan, N.A. Thu, P.K.H. Chow, Yttrium-90 microspheres: a review of its emerging clinical indications, Liver Cancer, 4 (2015) 6–15.
[94] H. Suzuki, Y. Sasaki, Y. Sugo, A. Apichaibukol, T. Kimura, Extraction and separation of Am(III) and Sr(II) by *N,N,N′,N′*-tetraoctyl-3-oxapentanediamide (TODGA), Radiochim. Acta, 92 (2004) 463–466.
[95] S. Dutta, P.K. Mohapatra, Studies on the separation of ^{90}Y from ^{90}Sr by solvent extraction and supported liquid membrane using TODGA: role of organic diluent, J. Radioanal. Nucl. Chem., 295 (2013) 1683–1688.
[96] S. Dutta, D.R. Raut, P.K. Mohapatra, Role of diluent on the separation of ^{90}Y from ^{90}Sr by solvent extraction and supported liquid membrane using T2EHDGA as the extractant, Appl. Radiat. Isot., 70 (2012) 670–675.

[97] R. Kumar, S.A. Ansari, P. Kandwal, P.K. Mohapatra, Selective permeation of ^{90}Y from a mixture of ^{90}Y/^{90}Sr through diglycolamide impregnated supported liquid membranes, Appl. Radiat. Isot., 170 (2021) 109604, doi: 10.1016/j.apradiso.2021.109604.
[98] P.K. Mohapatra, D.R. Raut, M. Iqbal, J. Huskens, W. Verboom, Separation of carrier-free ^{90}Y from ^{90}Sr using flat sheet supported liquid membranes containing multiple diglycolamide-functionalized calix[4]arenes, Supramol. Chem., 28 (2016) 360–366.
[99] V.G.J. Rodgers, S.F. Oppenheim, R. Datta, Correlation of permeability and solute uptake in membranes of arbitrary pore morphology, AlChE J., 41 (1995) 1826–1829.
[100] A.J.B. Kemperman, D. Bargeman, T.V.D. Boomgaard, H. Strathmann, Stability of supported liquid membranes: state of the art, Sep. Sci. Technol., 31 (1996) 2733–2762.
[101] D.S. Lakshmi, P.K. Mohapatra, D. Mohan, V.K. Manchanda, Uranium transport using a PTFE flat-sheet membrane containing alamine 336 in toluene as the carrier, Desalination, 163 (2004) 13–18.
[102] M. Sugiura, M. Kikkawa, S. Urita, Effect of plasticizer on carrier-mediated transport of zinc ion through cellulose triacetate membranes, Sep. Sci. Technol., 22 (1987) 2263–2268.
[103] A.J. Schow, R.T. Peterson, J.D. Lamb, Polymer inclusion membranes containing macrocyclic carriers for use in cation separations, J. Membr. Sci., 111 (1996) 291–295.
[104] S.C. Lee, J.D. Lamb, M.H. Cho, C.H. Rhee, J.S. Kim, A lipophilic acyclic polyether dicarboxylic acid as Pb^{2+} carrier in polymer inclusion and bulk liquid membranes, Sep. Sci. Technol., 35 (2000) 767–778.
[105] S.A. Ansari, P.K. Mohapatra V.K. Manchanda, Cation transport across plasticized polymeric membranes containing *N,N,N',N'*-tetraoctyl-3-oxapentanediamide (TODGA) as the carrier, Desalination, 262 (2010) 196–201.
[106] B. Mahanty, P.K. Mohapatra, D.R. Raut, D.K. Das, P.G. Behere, M. Afzal, Novel polymer inclusion membranes containing T2EHDGA as carrier extractant for actinide ion uptake from acidic feeds, Radiochim. Acta, 103 (2015) 257–264.
[107] D.R. Raut P.K. Mohapatra, A novel PVC based polymer inclusion membrane containing TODGA as the extractant for pre-concentration of americium from acidic feed solutions, Sep. Sci. Technol., 48 (2013) 2499–2505.
[108] B. Mahanty, P.K. Mohapatra, D.R. Raut, D.K. Das, P.G. Behere, M. Afzal, Comparative evaluation of actinide ion uptake by polymer inclusion membranes containing TODGA as the carrier extractant, J. Hazard. Mater., 275 (2014) 146–153.
[109] B. Mahanty, P.K. Mohapatra, D.R. Raut, D.K. Das, P.G. Behere, M. Afzal, Comparative evaluation of polymer inclusion membranes containing several substituted diglycolamides for actinide ion separations, J. Membr. Sci., 501 (2016) 134–143.
[110] B. Mahanty, P.K. Mohapatra, D.R. Raut, D.K. Das, P.G. Behere, M. Afzal, W. Verboom, Polymer inclusion membrane containing a tripodal diglycolamide ligand: actinide ion uptake and transport studies, Ind. Eng. Chem. Res., 55 (2016) 2202–2209.
[111] B. Mahanty, P.K. Mohapatra, D.R. Raut, D.K. Das, P.G. Behere, M. Afzal, W. Verboom, Polymer inclusion membrane containing a diglycolamide-functionalized calix[4]arene for actinide ion uptake and transport, J. Membr. Sci., 516 (2016) 194–201.